VOLTAGES PRODUCED AT THE POLARIZED MERCURY-ELECTROLYTE INTERFACE

by

Robert C. Mania, Jr.

Dissertation submitted to the Graduate Faculty of the
Virginia Polytechnic Institute and State University
in partial fulfillment of the requirements for the degree of
DOCTOR OF PHILOSOPHY
in
Physics

APPROVED

R. F. Tipsword, Chairman

C. D. Williams

S. P. Bowen

T. E. Leinhardt

A. L. Ritter

August, 1981

Blacksburg, Virginia

ACKNOWLEDGEMENTS

I am very grateful to my advisor Dr. Ray F. Tipsword for the suggestion of this problem and for his ideas and guidance which have been invaluable in preparing this thesis.

I am thankful to Dr. Sam P. Bowen with whom I had many hours of fruitful discussions and for his interest in my work.

Finally, I wish to thank my wife, parents, and in-laws for the encouragement they have given me in pursuing this work.

TABLE OF CONTENTS

I. INTRODUCTION

Experiments on streaming potentials and electrocapillarity were first conducted in the nineteen hundreds. Recently, there has been a lot of interest in electrocapillarity effects for making accelerometer devices. However, due to the complexity of the electrical double layers at the interfaces and the difficulity in solving fluid dynamics problems, there still seems to be a lack of understanding of the mechanisms involved. The purpose of this investigation is to assist in the understanding of these processes.

Background

A number of studies have been carried out since the early 1950's on the electrical double layer and electrocapillarity. It was first reported by S. Ueda and collabarators in 1951-53[1] that, while studying surface electrical phenomena, they discovered what they called the U-effect. This work was later published in an English journal.[2]

The U-effect was seperated onto two distinct phenomena by Ueda et al., U-effect I and U-effect II. U-effect I was found to produce an A.C. potential of 0.1 to 1 millivolt across the tube when an electrolyte was made to oscillate, with respect to the glass capillary walls. A fine glass rod fixed to a stationary external support was inserted in one end to impede the liguid from following the oscillating capillary wall. The mechanical disturbance of the glass-electrolyte interface, along the capillary walls, produced an alternating voltage of the same frequency and having the same waveform as the mechanical

vibration. The effect was studied with 10^{-3} to 10^{-6} N salt solutions, and at frequencies from 60 hertz to 13.5 khz. U-effect II was produced by a fast periodic vibration of a glass capillary tube in which alternate drops of electrolyte (1N HCl) and mercury were placed. They used approximately 20 drops of mercury or about forty interfaces. They suggested that the Hg-HCl interfaces were distorted as the capillary tubes were vibrated. They assumed that the double layer formed at an interface acted as a capacitor whose charge remained constant but whose area changed. The amplitude of vibration was about a micron and frequencies ranged from 0.5 to 15 khz. The output voltage was found to be a linear function of the number of interfaces present. Typical voltage values were 10 to 70 millivolts. Ueda et al. also reported that for constant frequency the output voltage was proportional to the amplitude of vibration. Furthermore, for constant amplitude of vibration, the output voltage was found to vary as the square of the frequency.

Further work was done in 1954 by Eliot et al.[3] Capillary tubes were constructed containing 1 Normal sulfuric acid as the electrolyte and between 50 and 80 mercury drops. They reported that the output voltage was proportional to the acceleration, being linear from 0 to 0.015g. Also, they found that for a constant acceleration the output increased as the tube diameter decreased.

In 1954, Fain et al.[4] reported on their investigations of the U-effect II. They used sealed capillary tubes with one or two interfaces, between mercury and sulfuric acid, whose internal diameter was 0.7 mm. They also introduced an air gap into one end of the tube. The output voltage was found to be linearly dependent on the amplitude of the tube motion. The upper limit to the linear region depended upon frequency. The output voltage versus frequency curve had a peak, which they called the resonance frequency. The voltage above this frequency dropped to a fairly constant value. They attributed the variation of the resonance frequency from tube to tube to the physical structure of the tube. They explained their results, as did Ueda et al., as a capacitor whose area changed but the charge remained constant.

In 1957, Podolsky and his collaborators[5] reported a new phenomenon which they called the U-effect III. This effect was attributed to the relative motion of the drops with respect to the capillary walls. They explained it as follows: "The flow pattern causes an effective expansion of the forward interface and an effective contraction of the rear interface. As a result, a double layer distribution of charge which is uniform when there is no relative motion between the drop and the capillary becomes non-uniform when the drop moves. At the forward end the effective expansion leads to a reduction of the dipole moment density over the interface; at the rear interface the effective contraction causes an increase of the dipole moment density there. The

field of the non-uniform dipole moment distribution leads to an observable output voltage." Capillary tubes of 5 to 50 cm in length and up to 1.5 mm in diameter were used. Two to ten mercury drops and 1 normal sulfuric acid was used to perform the investigation. The output was proportional to the amplitude of the drop motion and for constant amplitude was proportional to the square of the frequency.

Tipsword et al.[6] reported in 1976 that the output voltage was dependent upon the acceleration and the velocity of the drop. They interpreted the U-II and the U-III to be the same effect; that is, that while moving, the surface areas of the drop end become distorted while the number of dipoles remain fixed.

Kotowski et al.[7] reported in 1979 about the usefulness of electrocapillary elements as accelerometers. They show that replacing a solution of electrolyte by its solution in a gel increases the resonance frequency and allows a more extended use of such systems as measurement devices. Their model is the same basic one used by Ueda et al. They adjust the electrolyte until the system's impedance is mainly capacitative. They then obtain the result that the output voltage is proportional to the acceleration of the system.

Statement of the Problem

When a mercury drop is placed in contact with an electrolyte in a capillary tube, a double layer having an equilibrium dipole moment density is formed over each end of the drop. (A description of the formation of the double layer is given in Appendix A.) When the mercury and the capillary tube are moved relative to each other a voltage is developed between the ends of the tube.

Two different explanations were proposed to explain this voltage. Ueda[2] et al and Fain[4] et al. found that changes in the area of the interfaces cause the effect, while Podolsky[5] et al. claim that differences in charge density, brought on by the movement of the mercury, cause the voltage. Tipsword et al.[6] found that the U-II and U-III effects are the same effect; that is, the output voltage is due to the distortion of the surface areas of the two ends of the moving mercury drop, while the number of dipoles across each interface remains fixed.

The problem to which this thesis is directed is the explanation of the physical origin of the U effect and the quantitative application of that explanation.

As in the work of Tipsword et al.[6], the drop was given a finite displacement. This particular method allows one to investigate the voltage output as the drop is accelerated and decelerated. This method also allows an examination of the voltage in a transient or

relaxation mode. By using this method the phase problem associated with the periodic vibration method is avoided. One is also allowed to monitor the voltage as the drop's surface goes back into equilibrium after the bulk motion has stopped.

II. EXPERIMENTAL TECHNIQUES

The apparatus was designed to give the mercury-electrolyte interface a finite displacement inside the capillary tube. Advantages of this method over the A.C. techniques is that the phase problem associated with the other method is avoided. Experiments with single drops of mercury, varying in lengths and position in the tube with respect to the electrodes, were carried out at room temperature.

Preparation of Tubes

The capillary tubes were made of pyrex glass, having a precision-bored internal diameter of 1.0mm. At each end of the tubes is a pyrex glass cup of 0.7cm internal diameter which gives the tubes a dumb-bell shape with both ends open (see figure 1). Cleaning of the tubes was done by running nitric acid through them and rinsing them with distilled water; they were then dried at 200°C. The electrolyte used is 1 Normal perchloric acid, which was obtained from Fisher Scientific Company and was diluted with distilled water. Triple distilled mercury from Bethlehem Apparatus Company was used in the experiment. The tubes contained a single drop of mercury with electrolyte on both sides. Teflon pistons were put in the glass cups to make the whole system rigid. Platinum electrodes were sealed in the tubes as shown in Figure 1. The output voltage was measured across these electrodes.

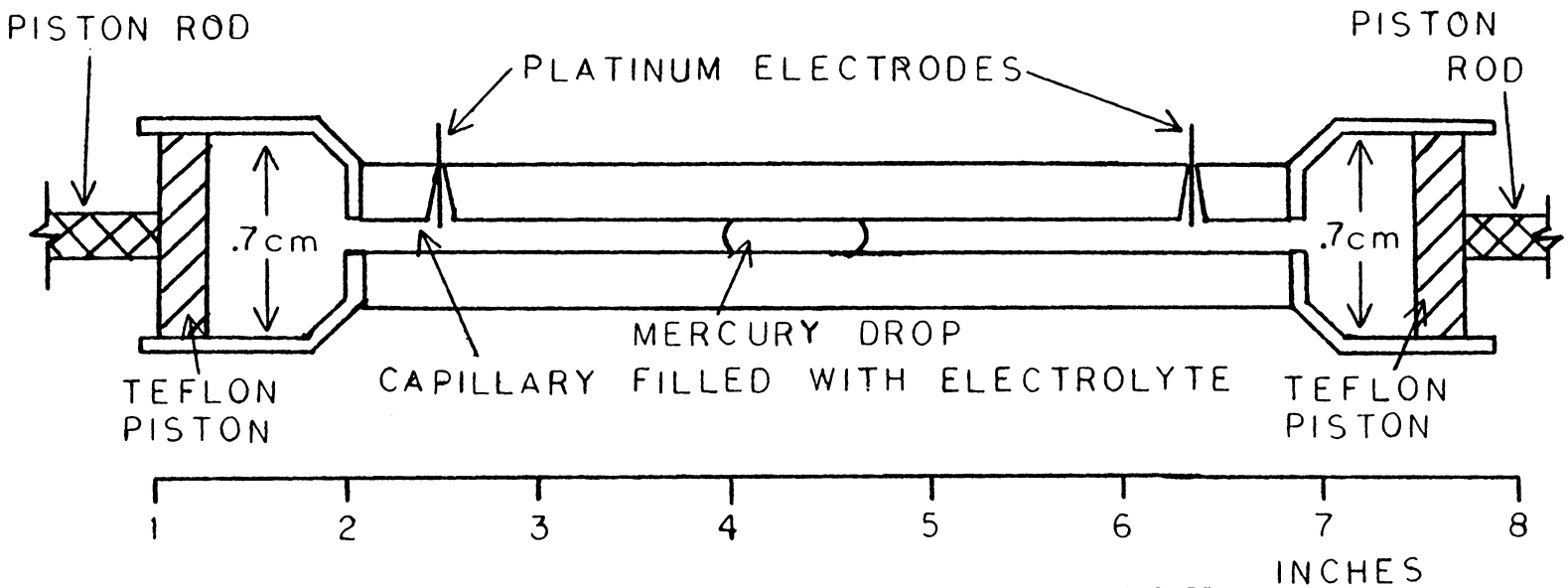

Fig. 1. Glass capillary tube in the shape of a dumb-bell.

Apparatus

Pictured in figure 2 is the apparatus used to accelerate the drops. The tubes were held in place by clamps A and the piston rods were attached by clamps to carriage C. A hammer with weights was attached to a lever and allowed to fall. The lever was attached to a screw which turned as the hammer fell. This screw moved the carriage to which the pistons were attached. Both pistons moved together which caused the electrolyte-mercury-electrolyte system to move as a unit. By dropping the hammer from different heights and with different masses attached to it, different acceleration and maximum velocities of the drop could be achieved since the frictional forces remained constant. The carriage was driven against seventy pounds per square inch of air pressure, which cushioned the mercury-electrolyte system and prevented the mercury drop from breaking apart when the system stopped. The voltage measured was displayed on a Tektronix memory scope, and the voltage versus time readings were taken from the oscilloscope. The distance the drop moved was measured using a traveling microscope. The time of fall of the hammer and the maximum velocity of the hammer were also measured. The maximum velocity of the hammer was measured by allowing a small aluminum plate of approximately $\frac{1}{2}$ cm in length to fall through a light beam. A timer started when the beam was interrupted and stopped when the beam became continuous again. The time of fall was measured in a

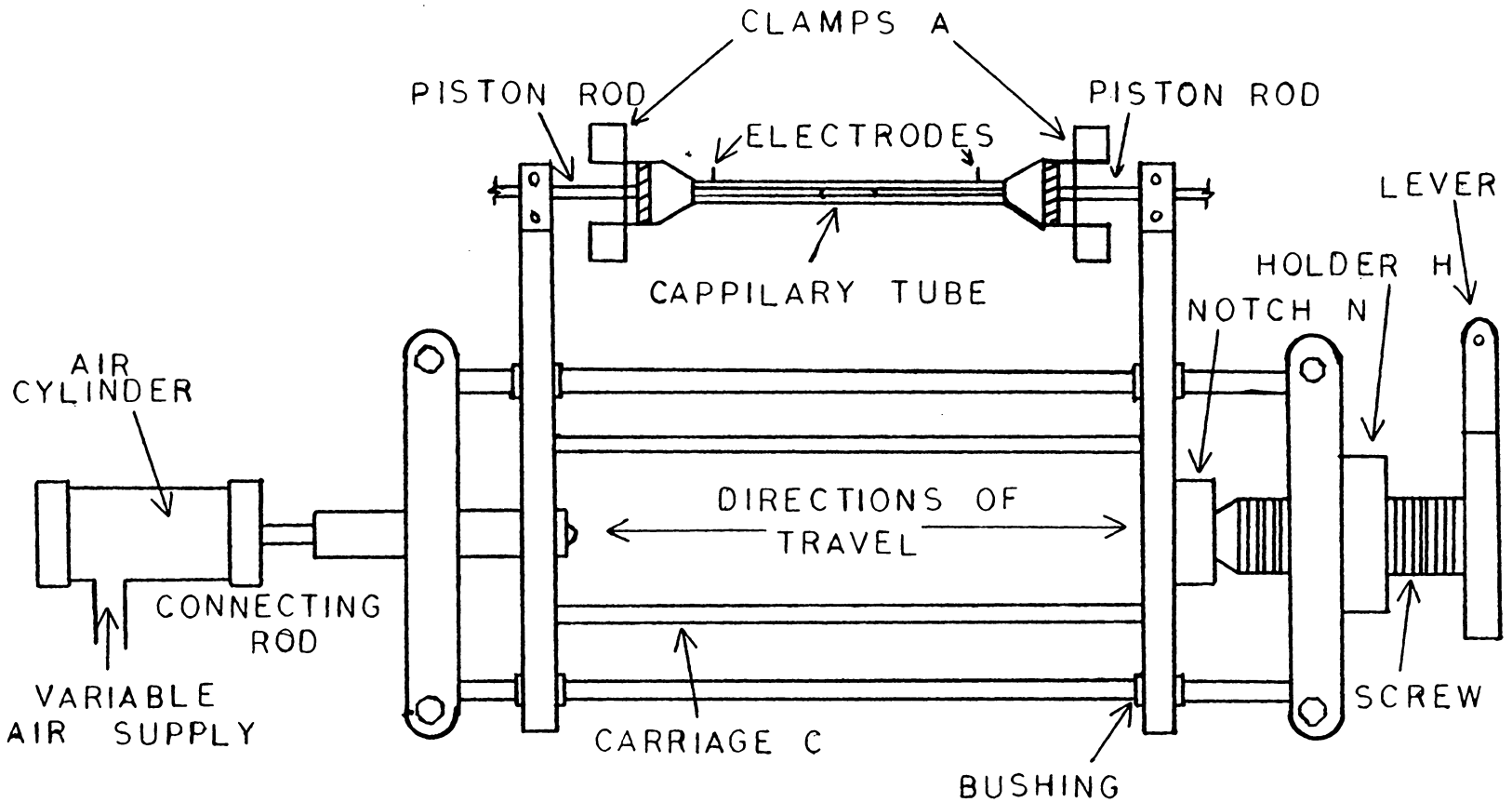

Fig. 2. Top view of the apparatus for giving the mercury drop a constant acceleration.

like manner. The mechanics of the apparatus is more completely described in Appendix D.

III. EXPERIMENTAL RESULTS

An output voltage was developed as a result of the movement of a mercury drop in the tube. This voltage was photographed as displayed on an oscilloscope and a typical trace is shown in figure 3. These observations seem to show several characteristics of the output voltage versus time that have not been previously reported. The trace can be divided into three distinct regions for analysis.

Region I is the portion of the curve in which the hammer is still accelerating as it fell. Measurements indicated that the hammer fell with a constant acceleration, thus imparting a constant acceleration to the drop. The output voltage versus time in this region exhibits a linear relation between the two. This relation is simply written as

$$V = kt$$

where V is voltage, t is time and k is a constant. The experimental value of k was between 1 and 5 volts per second for all drops. There was some variation due to the acceleration of the drop: the greater the acceleration (or force) the greater the value of k. It was also observed that is this region the voltage was linear with respect to the velocity of the drop (see figure 4).

Region II is the portion of the curve in which the hammer is being decelerated. The voltage decreased linearly with time in this section. A detailed analysis for this section was done since the mechanism for stopping the hammer could not be well controlled. Thus the voltage versus time varies consi erably since the stopping

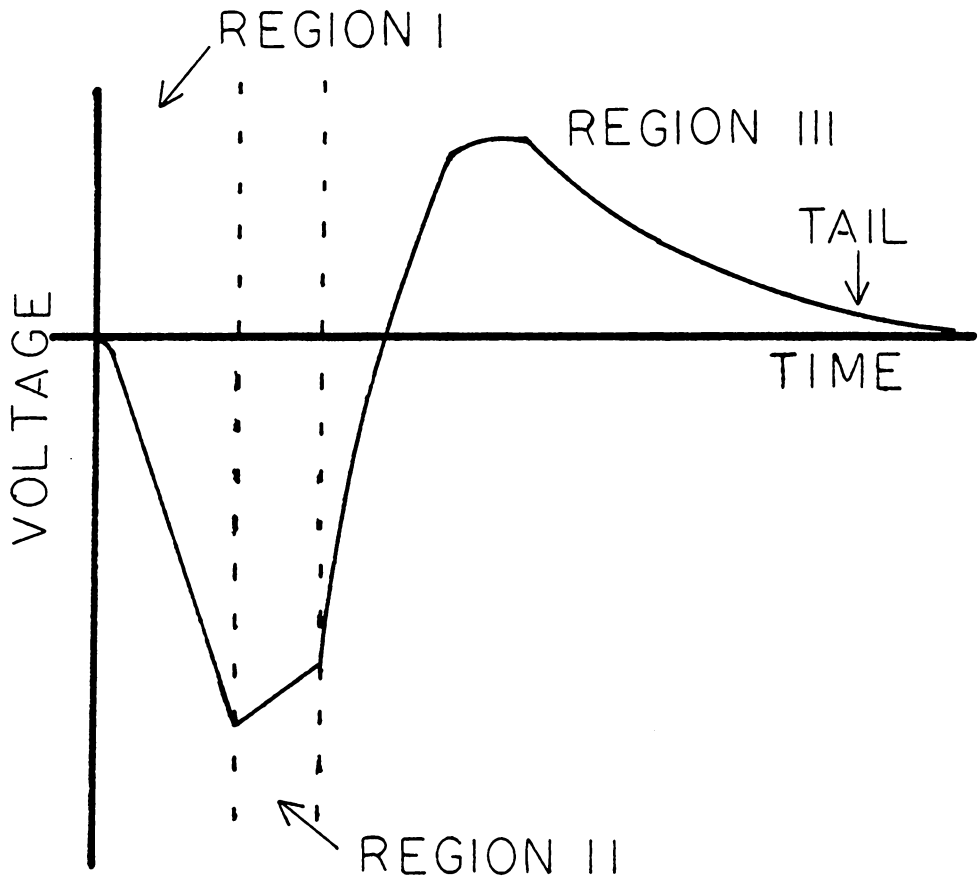

Fig. 3. Typical trace on oscilloscope.

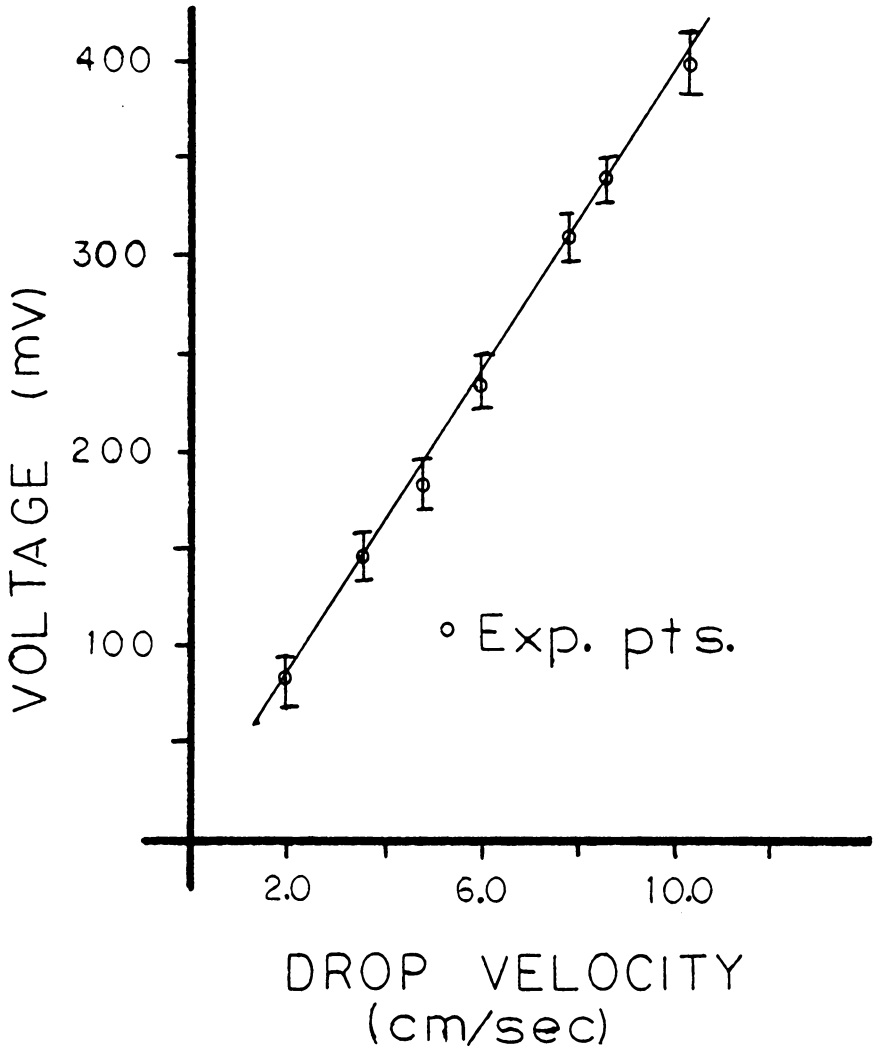

Fig. 4. Dependence of the output voltage on the drop velocity.

force varied greatly from data set to data set.

Region III of the curve corresponds to the bulk motion of the drop being stopped. This conclusion proceeds from several observations. First the hammer motion has stopped by this time. Secondly, since water is incompressible either the bulk motion of the drop has ceased also or fluid is moving around the drop. Two observations seem to indicate that the fluid is not moving around the drop: after each run when the hammer is slowly raised the drop comes back to essentially the same starting point, and, when dye was introduced in one end and the tube stood on end, giving accelerations large compared to that of the experiment, it took about 24 hours for the dye to move around the drop. This time is extremely long compared to that of the experiment. This indicates that when the hammer stopped the bulk motion of the drop also ceased.

The voltage can be fitted by the equation

$$V = Ae^{-t/\delta_1} + Be^{-t/\delta_2} \sinh\gamma t \quad ,$$

where δ_1, δ_2 are decay times and γ is a dampening term. The curve is the type obtained for an overdamped harmonic oscillator.[11]

When the time is long compared to δ_1, δ_2 and $1/\gamma$; the curve can be approximated by a pure exponential of the form

$$V = V_0 e^{-t/\delta_o} \quad ,$$

where δ_o is the effective decay constant. This approximation should

be valid for the tail portion of region III. The value of δ_o was determined for various lengths of the mercury drop. The values of $1/\delta_o$ versus drop length are plotted in figure 5.

Several sets of data were taken with two drops of mercury in the electrolyte. The voltage versus time plot has all the characteristics as that for one drop except that the output was double (to within 15 percent) that of one drop. This would imply that the voltage is proportional to the number of drops.

Finally, a measurement of the current through the electrolyte and mercury was taken for various known voltages across the system. The number of drops in the system was varied. From this information and the results of section IV, the electrochemical relaxation time can be calculated and compared to the mechanical decay times, the value of δ_o, that were measured for region III of the curve in figure 3. The electrochemical relaxation time turned out to be small (about 13 milliseconds) compared to the values of δ_o. This implies the effects being studied here represent a slower phenomena than the electrochemical response of the interface and that the electrochemical state of the system can always be assumed to be approximately in equilibrium. The data are presented in figure 6, which indicates that the voltage divided by current initially increases linearly as the number of drops. (See page 29, section IV for more details.)

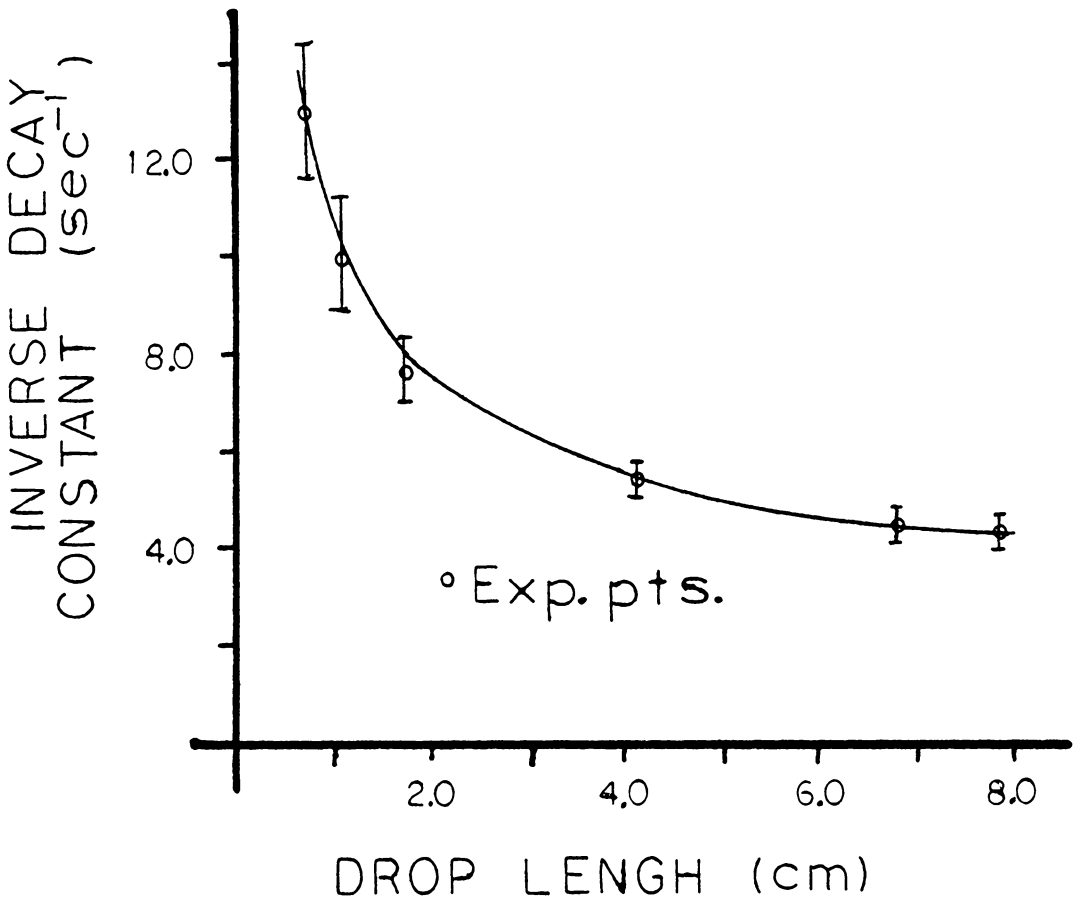

Fig. 5. Dependence of the inverse effective decay constant on the drop length.

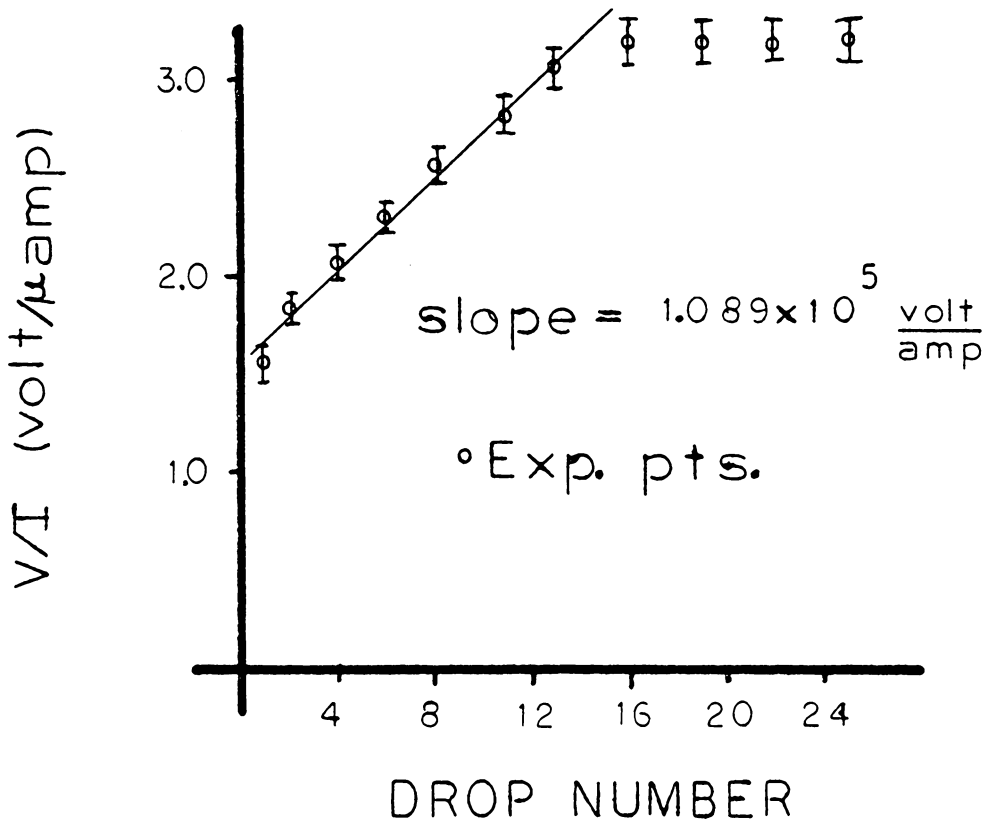

Fig. 6. Plot of voltage divided by current versus the the number of drops in the tube.

IV. MODEL

The model we are proposing to explain the experimental results is based on two assumptions. One is that the voltage follows the surface distortion; thus, the surface distortion needs to be calculated. The other is that the main contribution to the voltage is the Gibbs-Thompson[10] effect which relates how the surface affects the chemical potential and how the surface distortion changes the chemical potential.

Figure 7a shows a drop of mercury sandwiched between two sections of perchloric acid in a capillary tube. Perchloric acid was the electrolyte used in the experiment. Referring to figure 7b an approximate value for the thickness Δx of the curved layer between the mercury and the electrolyte can be obtained using the following approximation:

$$\begin{aligned} \triangle x_i &= r_i - \sqrt{r_i^2 - a^2} \\ &\cong r_i - r_i(1 - a^2/2r_i^2) \; ; \text{ where } a^2/2r_i^2 \ll 1 \\ &= a^2/2r_i \quad . \end{aligned}$$

Thus,

$$\triangle x_1 = a^2/2r_1$$

and

$$\triangle x_2 = a^2/2r_2$$

Using Landau's[8] results for the value of the curvature and the fact that the equilibrium pressure inside the mercury is higher than outside gives

$$P_1^o - P_2^o = 2\gamma/r_1$$

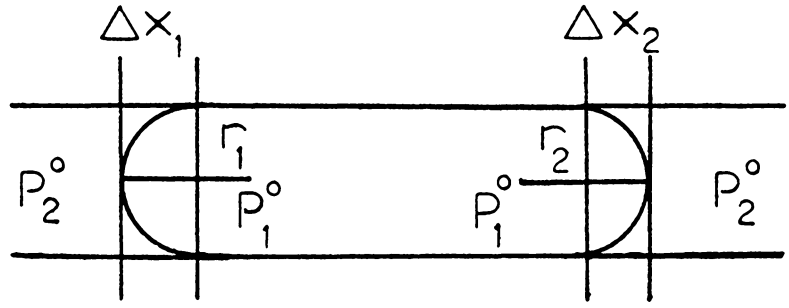

Fig. 7a. Mercury drop in tube showing variables used.

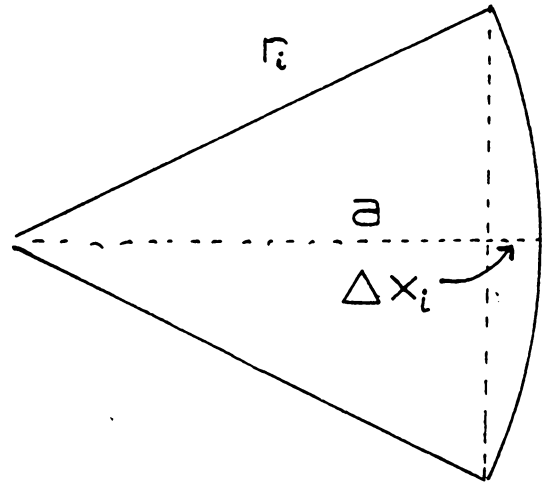

Fig. 7b. Expanded view of curved region of mercury drop showing variables used.

and $$P_1^o - P_2^o = 2\gamma/r_2 \quad ,$$

where γ is the surface tension and P_1^o, P_2^o are the equilibrium pressures. Using this and refering to figure 8 for the definition of the doubly subscripted quantities, an equation for Δx_{12} is obtained:

$$\Delta x_{12} = \frac{a^2}{4\gamma} (P_{21} - P_{11}) \quad .$$

This result can be obtained in a similar manner for Δx_{23}.

We start with the equation[9]

$$\rho \frac{\partial u}{\partial t} = \frac{\partial P}{\partial z} + \eta\left(\frac{1}{r}\frac{\partial u}{\partial r} + \frac{\partial^2 u}{\partial r^2} \right) \qquad (1)$$

where u is the velocity of flow, ρ the density of the material, η the viscosity and $\frac{\partial P}{\partial z}$ the pressure gradient across the fluid, and assuming that the pressure gradient is constant,

$$\frac{\partial P}{\partial z} = \frac{\Delta P}{\ell} = \text{constant} \ ,$$

and that the flow has achieved steady state so that

$$\frac{\partial u}{\partial t} = 0 \quad ,$$

and letting

$$u = u_o \left(1 - \frac{r^2}{a^2} \right) \quad , \qquad (2)$$

the following result is obtained upon substitution into equation (1):

$$u_o = \frac{a^2}{4\eta} \frac{\Delta P}{\ell} \quad .$$

Hence a pressure gradient is needed to obtain a flow, and the average

velocity, u_{ave}, is

$$u_{ave} = \frac{1}{\pi a^2} \int ur \, dr d\theta = \frac{u_o}{2} \quad .$$

Now, allowing a time variation of the velocity in conjunction with equations (1) and (2) and approximating the velocity by the average velocity, the following equation is obtained:

$$\rho \frac{\partial u_{ave}}{\partial t} + \frac{8\eta}{a^2} u_{ave} = \frac{\partial P}{\partial z} \quad .$$

Applying this equation to each segment of the tube shown in Figure 8, the following results are obtained:

$$\rho_1 l_1 \frac{\partial u_1}{\partial t} + \frac{8\eta_1 l_1 u_1}{a^2} = P_{10} - P_{11} \qquad (3a)$$

$$\rho_2 l_2 \frac{\partial u_2}{\partial t} + \frac{8\eta_2 l_2 u_2}{a^2} = P_{21} - P_{22} \qquad (3b)$$

$$\rho_3 l_3 \frac{\partial u_3}{\partial t} + \frac{8\eta_3 l_3 u_3}{a^2} = P_{23} - P_{11} \qquad (3c)$$

In the regions 1 and 3 the same electrolyte was used; hence, $\rho_3 = \rho_1$ and $\eta_3 = \eta_1$. Furthermore, since the mercury drop was in the center of the tube, $l_1 \cong l_3$. Putting

$$\Delta x_i = \frac{a^2}{2r_i} \quad \text{and} \quad \frac{2\gamma}{r_i} = \Delta P$$

into

$$\Delta x_{12} = (x_2 - \frac{l_2}{2}) - (x_1 + \frac{l_1}{2})$$

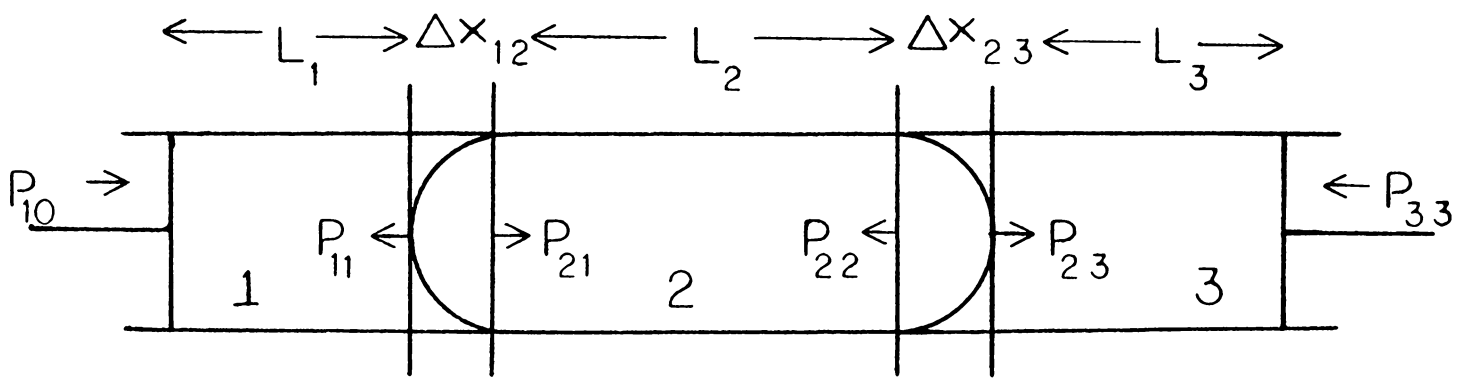

Fig. 8. View showing mercury drop sandwiched between two layers of electrolyte with the pressures across the drop labled as used in the model.

and

$$\Delta x_{23} = (x_3 - \frac{\ell_3}{2}) - (x_2 + \frac{\ell_2}{2})$$

the following relations are obtained:

$$P_{22} - P_{23} = \frac{-4\gamma}{a^2}(x_3 - x_2 - (\ell_2 + \ell_3)/2)$$

$$P_{21} - P_{11} = \frac{-4\gamma}{a^2}(x_2 - x_1 - (\ell_1 + \ell_2)/2) .$$

Substituting these results into equations (3) and dividing through by the appropriate $\rho\ell$ product, the following dynamic equations are obtained:

$$\dot{u}_1 + \frac{u_1}{\delta_1} = \frac{P_{23} - P_{33}}{\rho_1 \ell_1} \equiv N_1 \qquad (4a)$$

$$\dot{u}_3 + \frac{u_3}{\delta_1} = \frac{P_{10} - P_{11}}{\rho_1 \ell_1} \equiv N_3 \qquad (4b)$$

$$\dot{u}_2 + \frac{u_2}{\delta_2} + 2\beta y_2 - \beta y_3 - \beta y_1 = \frac{P_{11} - P_{23}}{\rho_2 \ell_2} \equiv N_2 \qquad (4c)$$

where

$$\beta = \frac{4\gamma}{\rho_2 \ell_2 a^2} , \qquad 1/\delta_1 = \frac{8\eta_1}{\rho_1 a^2}$$

$$1/\delta_2 = \frac{8\eta_2}{\rho_2 a^2} , \qquad y_1 = x_1 - (\ell_1 + \ell_2)/2$$

$$y_2 = x_2 , \qquad y_3 = x_3 - (\ell_2 + \ell_3)/2 .$$

These are the equations for coupled harmonic oscillators with damping. These equations can be solved using Laplace Transform methods. Their solution is shown in Appendix B.

In this model the voltage is assumed to be proportional to the distortion of the surfaces. Measuring the distortion by $y_{32} - y_{21}$ one obtains

$$V \propto y_{32} - y_{21} ,$$

and taking the solution shown in Appendix B, the output voltage is

$$V = Ae^{-t/\delta_1} + Be^{-t/2\delta_2} (\sinh\gamma t + C \cosh\gamma t). \qquad (5)$$

This equation gives the voltage output as a function of time after the bulk motion of the drop has stopped. The hyperbolic sine term is what is expected for an overdamped harmonic oscillator as given by Paul C. Matrin.[11] The other terms come from the fact that the equations represent coupled harmonic oscillators. The constants A, B, and C are functions of the decay constants, the viscosity and density of the material, and the overcoupling between the surface distortion and the voltage. γ is a constant which depends on the surface tension at the interface and on the density and length of the mercury drop plus the value of δ_2.

In order to fit the experimental data, the relationship between δ_1 and δ_2 is utilized:

$$\frac{\delta_2}{\delta_1} = \frac{\dfrac{8\eta_1}{\rho_1 a^2}}{\dfrac{8\eta_2}{\rho_2 a^2}} = \frac{\eta_1 \rho_2}{\eta_2 \rho_1} \qquad (6)$$

After substitution of the values of the viscosities and the densities equation(6)gives

$$\frac{\delta_2}{\delta_1} = 6.9 \ .$$

This indicates that the δ_1 exponential term decays quickly compared to the δ_2 term, as it should to fit the curve in region III.

On the tail of the curve, the voltage is assumed to to be a pure exponential of the form

$$V = Ae^{-t/\delta_o} \ .$$

Equation (5) can be expanded after ignoring the exponential with δ_1; one obtains for δ_o ,

$$\frac{1}{\delta_o} = \frac{1}{2\delta_2}(1 - \gamma) = \frac{1}{2\delta_2}\left[a - \sqrt{1 - \frac{d}{\ell_2}}\right] \qquad (7)$$

where d is a constant. This gives the type of curve needed to explain the data for inverse period versus drop length.

Equation (4) can also be solved during the period of acceleration, that is, when the bulk motion of the drop is not zero as already discussed. After expanding the solution as in Appendix B, one obtains

$$V = -ct \ ,$$

where V is voltage, t is time and c is a constant. This expansion is felt to be justified since the time is small compared to the decay times of the experiment. Hence, the exponentials were expanded and the lowest order terms kept. This term turns out to be linear in time, which matches the experimental results. A comparison between the theoretical and experimental parameters is given in the analysis.

In Appendix E is reviewed the basic chemistry and thermodynamics of the mercury-acid interface. The experimental results are due to one or both of the following processes: the mechanical (viscous) dampening of the motion, and the electrochemical readjustment of the overpotential to the new equilibrium values. In the model the first process is taken as the major effect (as verified by experiment) and the second is assumed to happen quite fast compared to the decay times of the voltage seen in the experiment. It is known that in order to dissolve mercury one must shake the solution violently or wait a long period of time.[10] Thus the activation energy is large and the current i, is small. Using[10]

$$i = i_o \left[e^{\frac{\beta e \eta}{kt}} - e^{\frac{-\beta' e \eta}{kt}} \right] \ ,$$

assuming $\beta = \beta' = \frac{1}{2}$, and solving for η , one obtains

$$\eta = \frac{kT}{\beta e} \ln\left[\frac{i}{2i_o} + \sqrt{1 + \left(\frac{i}{2i_o}\right)^2}\right] .$$

This gives the potential across the interface as

$$V = \phi^o + \frac{kT}{\beta e} \ln\left[\frac{i}{2i_o} + \sqrt{1 + \left(\frac{i}{2i_o}\right)^2}\right]$$

where ϕ^o is determined by equilibrium properties according to

$$\phi^o = \frac{\Delta G'}{F} + \frac{RT}{F} \ln \frac{C^M_{Hg^o}}{C^M_{Hg^+}}$$

(see Appendix E). This $\Delta G'$ must contain the curvature effect discussed in appendix D. Thus,

$$\Delta G' = \Delta G^o + \frac{2\sigma K}{C^M_{Hg^o}} ,$$

where ΔG^o is the free energy difference when K=0. This gives the potential difference across one interface as

$$\phi^o = \frac{\Delta G^o}{F} + \frac{2\sigma K}{C^M_{Hg^oF}} + \frac{RT}{F} \ln \frac{C^M_{Hg^o}}{C^S_{Hg^+}}$$

$$= \Delta\phi_o + \frac{2\sigma K}{C^M_{Hg^oF}} ,$$

where $\Delta\phi_o$ is the term not depending on the radius of curvature. The voltage measured is the difference between the voltage from distortion due to each interface. This voltage is

$$\Delta V = \Delta\phi^L_o + \frac{2\sigma K^L}{C_{Hg^F}} - \Delta\phi^R_o - \frac{2\sigma K^R}{C_{Hg^F}}$$

$$= \frac{2\sigma}{C_{Hg^F}} (K^L - K^R) .$$

Using $C_{Hg}F = e/a^3$, where a is the lattice spacing of mercury and e is the charge of the electron, the voltage becomes

$$\Delta V = \frac{2\sigma a^3}{e} (K^L - K^R) \quad .$$

The reason the contribution to the voltage due to the electrochemical overpotential readjusting to a new equilibrium value is assumed to be small is that the relaxation time is short compared to the mechanical relaxation times of about 0.1 second. A value of the electrochemical relaxation time can be obtained as follows. By placing a small voltage across the tube, this voltage is

$$V = 2\eta_{Pt} + 2\eta_{Hg} \ ,$$

where η_{Pt}, η_{Hg} are the overpotentials of the Pt electrode and the mercury interfaces respectively. The factor of two comes in since there are two of each type of interface. Since

$$i = i_o \left[e^{\frac{\beta e \eta}{kT}} - e^{\frac{-\beta e \eta}{kT}} \right] \ ,$$

where β is assumed to be $\frac{1}{2}$ and the arguments of the exponentials are small, one obtains

$$i = \frac{e i_o}{kT} \eta \quad .$$

This gives for the voltage

$$V = \frac{2kT}{e i_o(Hg)} i + \frac{2kT}{e i_o(Pt)} i \ .$$

Assuming that the voltage for n drops is n times the voltage for one

drop, one obtains for the voltage divided by current

$$\frac{V}{i} = n \frac{2kT}{ei_o(Hg)} + \frac{2kT}{ei_o(Pt)} \quad .$$

By plotting V/i versus n, and using the slope, a value for $i_o(Hg)$ can be obtained. Bockris[10] gives a relationship between $i_o(Hg)$ and the electrochemical relaxation time as

$$\tau = \frac{kTC}{ei_o(Hg)} \quad ,$$

where C is the capacitance, T is the temperature, k is the Boltzmann constant and e is the electronic charge.

According to Bockris[10], page 1238 gives the value of $-\log i_o(Hg)$ as 12.3 for 1N H_2SO_4, for H_2 evolution, while our measurement of voltage and current across the interface in 1.5 N $HClO_4$ gives the value of $-\log i_o(Hg)$ as 6.4 This value of $i_o(Hg)$ gives a value of about 15 milliseconds for the electrochemical relaxation time, which time is short compared to the experimental times.

V. ANALYSIS

The output voltage versus time is shown in figure 3. The analysis will be done for each region of the curve separately starting with region III.

The model (see Appendix B) for region III of the curve gives the output voltage versus time as

$$V = Ae^{-t/\delta_1} + Be^{-t/2\delta_2}\left(\sinh\frac{\gamma t}{2\delta_2} + C\cosh\frac{\gamma t}{2\delta_2}\right) . \quad (5)$$

The assumption is made that in this region of the curve the bulk motion of the drop has stopped; and the drop, which is distorted in moving, is returning to equilibrium. In addition, the assumption is made that this return to equilibrium is a volume conserving oscillation. This assumption was made on account of the experiment with the dye and the observation that the drop returned to its initial position, as mentioned in section III. Thus, it is felt that the volume of the electrolyte remains constant and the surface oscillates in such a way as to allow this, as illustrated in figure 9. Figure 9 shows the drop's surface at two different times. The volume of the drop above the dashed lines equals the amount missing below the dashed line.

In equation (5) above, δ_1 depends on electrolyte properties, δ_2 and γ on mercury properties. Thus the first term in equation (5)

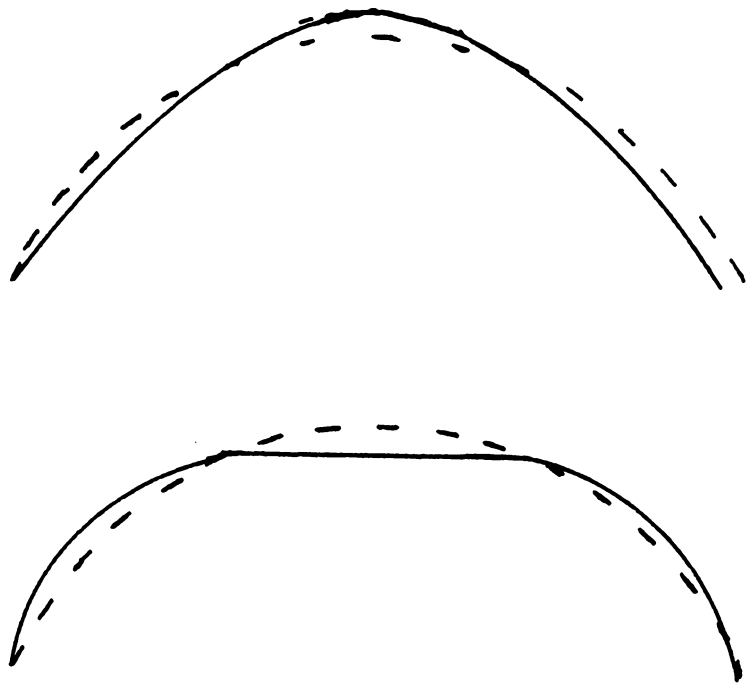

Fig. 9. A two dimensional view of the curved surface of the mercury drop at two different times. The dashed line is the equilibrium surface shape.

is determined by the electrolytic medium. The hyperbolic sine term (see Paul C. Martin[11]) is what is expected for an overdamped harmonic oscillator. The hyperbolic cosine term, as with the first term, occurs since the equations are coupled. Since this term depends on the properties of the mercury, the assumption is made that this term is the coupling of the two ends of the mercury through the drop itself. The model gives the parameter C in the equation as less than one. Equation (5) does roughly fit the experimental data with a finite value of C, though the smaller the value of C the better the fit. Since each end of the mercury drop oscillates in a volume conserving way, and assuming that the bulk of the mercury does not play a part in this oscillation, the value of C is taken to be zero. This then gives the voltage out versus time as

$$V = Ae^{-t/\delta_1} + Be^{-t/2\delta_2} \sinh\frac{\gamma t}{2\delta_2} \quad . \qquad (8)$$

The assumption that the two ends are not coupled through the mercury means that each interface can be treated as a sep rate harmonic oscillator. The equations for a two mass system (see Appendix G) are slightly different in the coupling, but they do give qualitative agreement.

In fitting equation (8) to the experimental data several parameters have to be evaluated. These parameters are δ_1, δ_2, A and B. A is the value of V for t = 0 (the starting point in region III). The model

gives two relationships between δ_1, δ_2 and γ; these are the value of the ratio of δ_1 to δ_2 and the value of the effective decay constant δ_o, for the tail region of the curve. All these parameters can be fitted to the data by observing the value of the voltage and time at two points other than the t = 0 point. In the conclusion the experimental and theoretical values of the key parameters will listed and discussed. Figure 10 shows a data set (the individual points) and a curve (solid line) using this model. In Appendix F is listed the other values for the model curves and experimental points. The values of all data points can be fitted within a few percent. This is better than the accuracy in reading the points from the photographs of oscilloscope traces.

No detailed analysis was done for region II of the curve. It was noted that the voltage versus time was linear and the magnitude decreased as the drop was decelerated.

The model also gives, for region I of the curve, the voltage output as a linear function of time; that is,

$$V = -c't \quad . \tag{7}$$

This value of c' can be evaluated simply by using the experimental points. The value of c' has also been calculated using the model. The comparison between these two values is made in the conclusion. The acceleration of the hammer and thus the drop were found to be independent of the velocity in this region (see figure 11). Figure

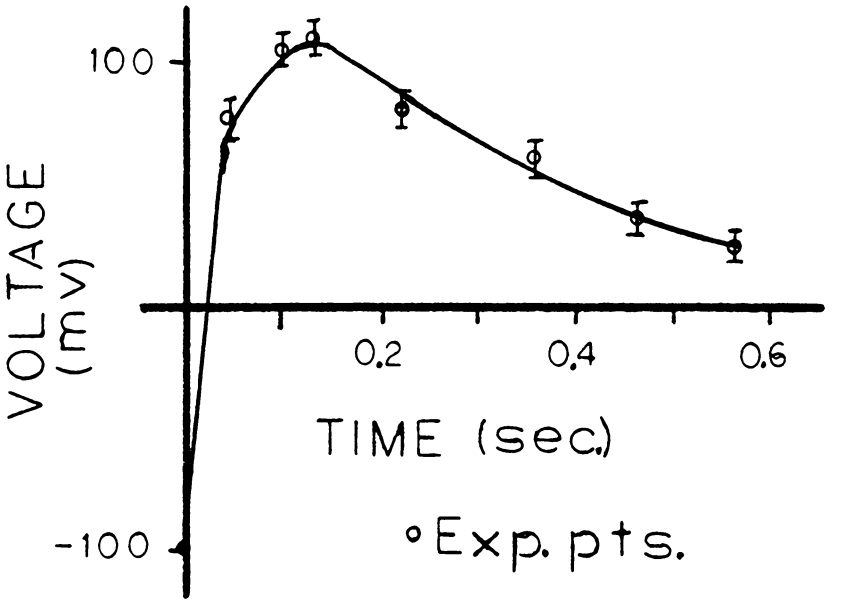

Fig. 10. Experimental points and model fit to the points for Region III of the curve (7.818 cm drop).

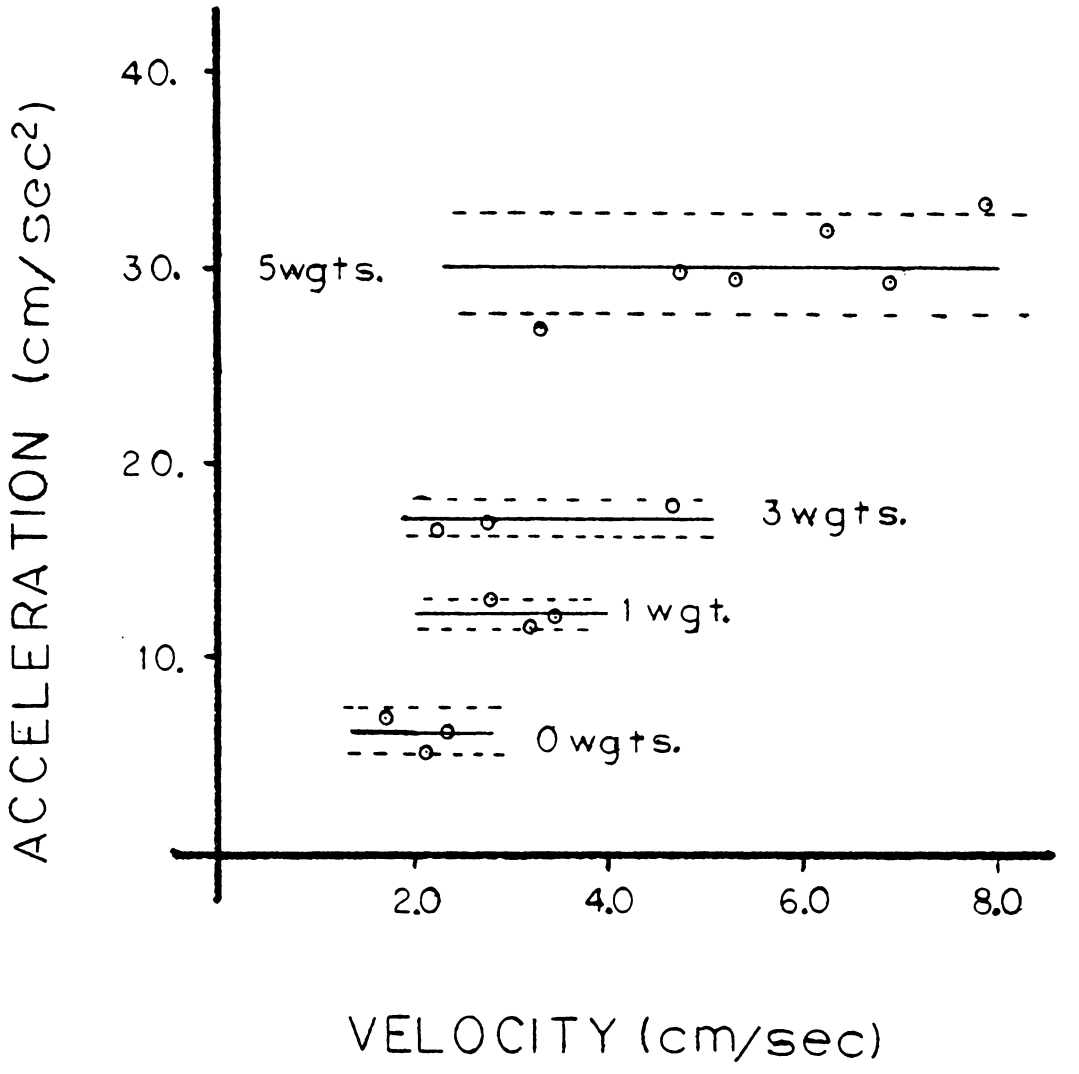

Fig. 11. Acceleration versus velocity for various number of accelerating weights. Solid line is the average value and the dashed line is the error margin.

11 shows the acceleration of the drop for different distances of fall (thus different velocities). This gives, for velocity versus time,

$$v = at \quad .$$

Solving for time from this equation and substituting into equation (7) gives

$$V = -\frac{c'}{a} v \quad .$$

Thus, while the drop is being accelerated, the voltage is linear in velocity (see figure 4).

VI. CONCLUSION

Comparison of Model Calculations and Experimental Results

Several parameters will be used to compare the model predictions with the experimental results. These parameters are the decay constant δ_2, the slope c of the voltage versus time in region I, and the parameters in equation (7) which describes the effective decay constant δ_o as a function of drop length in region III.

Because of the following assumptions in the model it is felt that the model can only be used to calculate the values of these parameters to within an order of magnitude: 1) the flow is laminar, 2) the surface tension for mercury-perchloric acid interface is identical to that of a water-mercury interface, 3) the interface is spherical even when moving, 4) the magnitudes of the forces involved on the drop are not known in detail and are only crudely estimated, 5) only the average velocity is used in the model, thus neglecting any radial dependence in the velocity, 6) the charge density in the interface is not known and the value assumed is that of one electron per atom of mercury in the drop for the interface, and 7) the interface consists of both acid and mercury.

The errors in the experimental values of the parameters come from the measurements of the voltage and time from the oscilloscope. The experimental data refer to six drop lengths of mercury with 24 data sets for each plus additional data sets giving a total of

more than 144 data sets. The data were reproducible only to within ten percent over most of the curve. However, in the tail region of the curve the voltage was reproducible to only twenty percent.

Looking at the value of the ratio of δ_2 as determined in the appendices one obtains

$$\frac{\delta_2)_{th}}{\delta_2)_{exp}} = 4.3 \pm 1.3 \quad .$$

To determine $\delta_2)_{exp}$ the experimental value of δ_o is determined first, using two points from the tail of the curve. Then region III of the curve is fit by a pair of exponentials of the form

$$V = B\left(e^{-t/\delta_o} - e^{-t/\delta_o} e^{-2xt} \right)$$

where x amd B is varied to obtain the best fit. The chi squared of this fit ranges from 4 to 10 for the different drop lengths. Since there are 24 points for each drop length, it is felt that the fit is very good. Then the value of $\delta_2)_{exp}$ is given by

$$1/\delta_2 = 1/\delta_o + x \quad .$$

The value of δ_o is calculated from

$$\delta_o = t/\ln(V_o/V) \quad .$$

The value of δ_o is fairly insensitive to the ratio of V_o to V due to the logarithmic dependence of δ_o on this ratio. The 20 percent error in the voltage gives an error of about 20 percent in the value of δ_o,

and thus δ_2. The error in the value of the ratio can be accounted for by the error in reading the values of the voltage and time and the propagation of these errors in the subsequent calculations for δ_o and δ_2. The experimental values are within an order of magnitude of the model values.

The equation for the effective decay constant versus drop length is evaluated by using two points as a starting place to calculate the values of a and b in equation (7). The fit was so good from the use of these two points that no variation of the parameters was needed to fit the points. The ratio of the theoretical values to the experimental values are

$$\frac{a_{exp}}{a_{th}} = 1.2 \pm 0.1$$

and

$$\frac{b_{th}}{b_{exp}} = 800 \pm 20 \quad .$$

The reliability of the fit can be checked by calculating the chi squared of the points. This calculation is made by obtaining the deviation from the best fit value and squaring, then dividing by the square of the estimated error. The value of the chi squared for the 144 points used is 24. It is felt that this implies that the fit is good.

Equation (7) can be manipulated into the form

$$\sum = 1 - \left(a - 2\delta_{2/\delta_o} \right)^2 = b/\ell \quad .$$

The quantity $\sum$ should be a linear function of the inverse drop length, as shown in figure 12.

The values of a_{exp} and a_{th} agree to within the accuracy of the model. The small discrepancy can be explained by the error in the measurement of voltage and time read with the oscilloscope. However, the ratio of b_{th} to b_{exp} is off much more than can be explained by measurement errors. The theoretical value of b depends on the density, viscosity, and the surface tension. This parameter is also dependent on what is happening in the interface. We have ignored the fact that both mercury and acid exist in this region. Some adjustment of the surface tension could bring the value of this ratio down, but not enough to be close to one. It is thus felt that the model is deficient for use in calculating the value of this parameter.

Lastly, the value of the slope in region I can be calculated. This can be done experimentally by just measuring the peak voltage and time to attain this peak. The ratio of the experimetnal value of the slope to the theoretical value is

$$\frac{\left.\frac{\Delta V}{\Delta t}\right)_{exp}}{\left.\frac{\Delta V}{\Delta t}\right)_{th}} = 23 \pm 6 \quad .$$

The accuracy of the experimental value for the slope is not better than twenty percent. In determining the experimental value of the slope the voltage is divided by a small value of time. This value of time, reliability to twenty percent, causes a similar error in

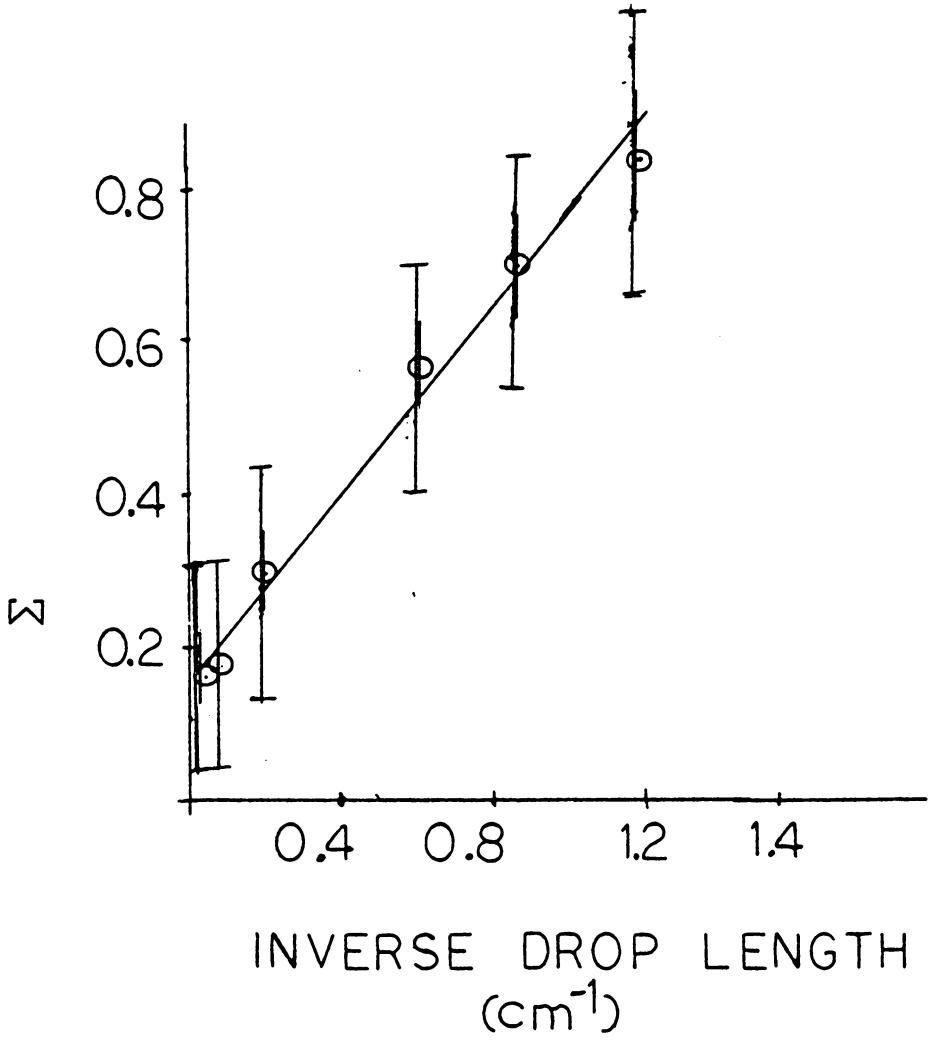

Figure 12. Shows the dimensionless quantity versus the inverse drop length which should be linear.

the slope. When calculating the theoretical value of the slope several assumptions are made. These assumptions are assumptions about the magnitude of the forces on both ends of the drop, the charge density in the interface, and the value of the surface tension. The value of the forces used was the pressure supplied by the air. The surface tension is assumed to be that of a water-mercury interface. Finally, the charge density in the interface is assumed to be one electron per unit cell of mercury. In examining these three assumptions the first two are felt to be reasonable while the other is poor. The charge density is considered to be too large. Adjusting this does alter the ratio of the value of the slopes in region I correctly.

In conclusion the values of δ_2, a_{th} and $\Delta V/\Delta t$ are within acceptable limits to the respective experimental values. However, the value of b_{th} can not be easily corrected and represents a real failure of the model.

It is felt however that the model does qualitatively explain the experimental data and can be used to give an order of magnitude for most of the results seen. Thus, it is felt that the model is semi-quantitavely correct.

In contradiction to the theory of Kotowski et al.[7] which predicts that the voltage output for the mercury drops moving in the presence of an electrolyte depends on the acceleration of the drop, we find that the voltage depends on the velocity of the drop. The experimental

method used in this work avoids the phase problem which makes the interpretation of results difficult for the A.C. methods.

The reproducibility of the experiment was mostly within ten percent. The glass capillary tubes were of precision bore and of small error. The errors are in finding the velocity and acceleration of the drop and in reading the voltage and time off the oscilloscope. Any further errors in the experimental values could come from the impurities in the mercury and perchloric acid and preparing the tubes in air rather than a vacuum. Impurities on the surface of the drops can affect the results dramatically.[12]

The experiment does also suggest that the Gibbs-Thompson affect is the mechanism for the coupling of the voltage to the distortion of the drop through the radius of curvature.

Suggestions for further experiments would be to check the idea that the voltage comes from an excited surface mode by using lasers to measure the time dependent doppler effect to obtain the profile of the surface of the drop as it moves. A more exact study of the hydrodynamics could also be attempted.

Appendix A

Electrical Double Layer at Interfaces.[10]

The electrical double layer is an array of charged particles and orientated dipoles thought to exist at every interface. For a metal-electrolyte interface, it is thought that the double layer consists of a layer of electrons on the metal, then a layer of water, and then a layer of ions in an abnormally high concentration, falling to normal with distance from the surface.

The study of interfaces is usually done with a mercury-solution interface since, mercury being a liquid, its surface is easily cleaned and free from mechanical strains. The low chemical activity and the large hydrogen overvoltage of mercury are also desirable properties. The latter helps prevent the solvent from being reduced to form hydrogen.

Appendix B

Solving Model Equations

The following model equations need to be solved:

$$\dot{u}_1 + \frac{u_1}{\delta_1} = N_1 \tag{1}$$

$$\dot{u}_2 + \frac{u_2}{\delta_2} + \beta(2y_2 - y_1 - y_3) = N_2 \tag{2}$$

$$\dot{u}_3 + \frac{u_3}{\delta_1} = N_3 \quad . \tag{3}$$

Taking the Laplace transforms (see Appendix C) with

$$\ddot{y}(s) = s^2 y(s) - sy(0) - y'(0)$$

and

$$\dot{y}(s) = sy(s) - y(0) \ ,$$

equation 1 becomes

$$y_1(s)\left[s^2 + \frac{s}{\delta_1}\right] = N_1' + y_1'(0) + y_1(0)\left[s + \frac{1}{\delta_1}\right]$$

equation 2 becomes

$$y_2(s)\left[s^2 + \frac{s}{\delta_2} + 2\beta\right] - \beta y_1(s) - \beta y_3(s) = N_2' + y_2'(0) + y_2(0)\left[s + \frac{1}{\delta_2}\right]$$

equation 3 becomes

$$y_3(s)\left[s^2 + \frac{s}{\delta_1}\right] = N_3' + y_3'(0) + y_3(0)\left[s + \frac{1}{\delta_1}\right] \quad .$$

Therefore a matrix equation can be set up in the form

$$M(s)\ Y(s) = N'(s) + Y'(0) + R(s)\ Y(0)$$

where

$$M(s) = \begin{bmatrix} s(s + \frac{1}{\delta_1}) & 0 & 0 \\ -\beta & s^2 + \frac{s}{\delta_2} + 2 & -\beta \\ 0 & 0 & s(s + \frac{1}{\delta_1}) \end{bmatrix}$$

$$N(s) = \begin{bmatrix} N_1' \\ N_2' \\ N_3' \end{bmatrix} \qquad R(s) = \begin{bmatrix} s + \frac{1}{\delta_1} & 0 & 0 \\ 0 & s + \frac{1}{\delta_2} & 0 \\ 0 & 0 & s + \frac{1}{\delta_1} \end{bmatrix}$$

$$Y(0) = \begin{bmatrix} y_1(0) \\ y_2(0) \\ y_3(0) \end{bmatrix} \qquad Y'(0) = \begin{bmatrix} y_1'(0) \\ y_2'(0) \\ y_3'(0) \end{bmatrix} \qquad Y(s) = \begin{bmatrix} y_1(s) \\ y_2(s) \\ y_3(s) \end{bmatrix} .$$

These can be solved for Y(s) by finding the inverse of M(s) and multiplying through by this inverse to get an equation of the form

$$Y(s) = M^{-1}(s)\, N(s) + M^{-1}(s)\, Y'(0) + M^{-1}(s)\, R(s)\, Y(0)$$

where

$$M^{-1}(s) = \begin{bmatrix} \frac{1}{s(s + \frac{1}{\delta_1})} & 0 & 0 \\ \frac{\beta}{s(s + \frac{1}{\delta_1})(s^2 + \frac{s}{\delta_2} + 2\beta)} & s^2 + \frac{s}{\delta_2} + 2\beta & \frac{\beta}{s(s + \frac{1}{\delta_1})(s^2 + \frac{s}{\delta_2} + 2\beta)} \\ 0 & 0 & \frac{1}{s(s + \frac{1}{\delta_1})} \end{bmatrix}$$

The zeros of M are the poles of M^{-1} for use in taking the inverse transforms and getting the frequencies. Therefore,

$$M = s^2\left(s + \frac{1}{\delta_1}\right)^2\left(s^2 + \frac{s}{\delta_2} + 2\beta\right)$$

setting $M = 0$ implies

$$s = 0 \ , \ s = \frac{-1}{\delta_1}$$

and $$s = \frac{-1}{2\delta_2}\left(1 \pm \sqrt{1 - 8\beta\delta_2^2}\right) \ .$$

Defining $$\sqrt{1-8\beta\delta_2^2} = \gamma$$

gives $$s = 0, \ \frac{-1}{\delta_1} \ , \ \frac{-1}{2\delta_2}(1 + \gamma) \ .$$

When the hammer is moving, $Y'(0) = 0$ and $Y(0) = 0$ (that is in region I); when the hammer has stopped (region III), $N = 0$.

First, working with the case where the bulk motion of the drop has stopped (region lll), $N = 0$, one obtains

$$Y(s) = M^{-1}Y'(0) + M^{-1}R\,Y(0) \ .$$

This gives the following equations:

$$y_1(s) = \frac{\dot{y}_1(0)}{s\left(s + \frac{1}{\delta_1}\right)} + \frac{y_1(0)}{s}$$

$$y_2(s) = \frac{\dot{y}_2(0)}{s\left(s + \frac{1}{\delta_1}\right)} + \frac{y_3(0)}{s}$$

$$y_2(s) = \frac{\beta\ y_1'(0) + y_3'(0)}{s(s + \frac{1}{\delta_1})(s^2 + \frac{s}{\delta_2} + 2\beta)} + \frac{y_2'(0)}{s^2 + \frac{s}{\delta_2} + 2\beta}$$

$$+ \frac{\beta\ y_1(0) + y_3(0)}{s(s^2 + \frac{s}{\delta_2} + 2\beta)} + \frac{y_2(0)\ (s + 1/\delta_2)}{s^2 + \frac{s}{\delta_2} + 2\beta} \quad .$$

These equations can be solved (using Appendix C). First,

$$y_1(t) = y_1(0)\ I_1 + y_1'(0)\ I_2$$

$$= y_1(0) + y_1'(0)\ \delta_1(1 - e^{-t/\delta_1}) \quad .$$

Secondly,

$$y_3(t) = y_3(0)\ I_1 + y_3'(0)\ I_2$$

$$= y_3(0) + y_3'(0)\ \delta_1(1 - e^{-t/\delta_1}) \quad .$$

Lastly,

$$y_2(t) = \beta\left[y_1'(0) + y_3'(0)\right]\ I_6 + y_2'(0)\ I_3 + \beta\left[y_1(0) + y_3(0)\right] I_4 + y_2(0)\ I_5$$

$$= y_2'(0)\frac{2\delta_2}{\gamma} e^{-t/2\delta_2} \sinh\frac{\gamma t}{2\delta_2} + \frac{y_2(0)}{\gamma} e^{-t/2\delta_2}\left[\gamma\cosh\frac{\gamma t}{2\delta_2} + \sinh\frac{\gamma t}{2\delta_2}\right]$$

$$+ \beta\left[y_1(0) + y_3(0)\right]\left\{\frac{1}{2\beta} + \frac{4\delta_2^2\, e^{-t/2\delta_2}}{\gamma(\gamma^2 - 1)}\left[\gamma\cosh\frac{\gamma t}{2\delta_2} + \sinh\frac{\gamma t}{2\delta_2}\right]\right\}$$

$$+\beta\left[y_1'(0) + y_3'(0)\right]\left\{\frac{\delta_1}{2} - \frac{\delta_1^3\, e^{-t/\delta_1}}{(1 + \delta_1/\delta_2 + 2\beta\delta^2)}\right.$$

$$\left. + e^{-t/2\beta_2} \cosh\frac{\gamma t}{2\delta_2}\left[\frac{\delta_1^3}{(1 + \delta_1/\delta_2 + 2\beta\delta_1^2)} - \frac{\delta_1}{2\beta}\right]\right.$$

$$+ \frac{e^{-t/2\delta_2}}{\gamma} \sinh\gamma t \left[\frac{\delta_1^3 (1 - 2\delta_2/\delta_1)}{(1 + \delta_1/\delta_2 + 2\beta\delta_1^2)} - \frac{\delta_1}{2\beta} \right] \Bigg\} .$$

The deformation of the front end of the drop is given by $y_3 - y_2$ and the deformation of the back end of the drop is given by $y_2 - y_1$. The voltage out is assumed to be do the the difference between the deformation of the front and rear of the drop. this gives

$$V \propto (y_3 + y_1 - 2y_2).$$

Substituting the expressions for y_1 , y_2 and y_3, one obtains

$$V \propto \left\{ \frac{2\delta_1^3\beta\left[y_1'(0) + y_3'(0)\right]}{(1 + \delta_1/\delta_2 + 2\beta\delta_1^2)} - \delta_1 y_3'(0) - \delta_1 y_1'(0) \right\} e^{-t/\delta_1}$$

$$- 2e^{-t/2\delta_2} \cosh\gamma t \left[y_2(0) - \tfrac{1}{2}\left[y_1(0) + y_3(0)\right] - \frac{\delta_1}{2}\left[y_1'(0) + y_3'(0)\right] \right.$$

$$\left. + \frac{\delta_1^3 \left[y_1'(0) + y_3'(0)\right]}{(1 + \delta_1/\delta_2 + 2\beta\delta_1^2)} \right]$$

$$- \frac{2e^{-t/2\delta_2}}{\gamma} \sinh\gamma t \left[2\delta_2 y_2'(0) + y_2(0) - \tfrac{1}{2}\left[y_1(0) + y_3(0)\right] \right.$$

$$\left. - \frac{\delta_1}{2}\left[y_1'(0) + y_3'(0)\right] + \frac{\beta\delta_1^3 (1 - 2\delta_2/\delta_1) \left[y_1'(0) + y_3'(0)\right]}{(1 + \delta_1/\delta_2 + 2\beta\delta_1^2)} \right].$$

This can be rewritten as

$$V = Ae^{-t/\delta_1} + Be^{-t/2\delta_2}\left[\sinh\frac{\gamma t}{2\delta_2} + C\cosh\frac{\gamma t}{2\delta_2}\right].$$

where A, B, and C are constants representing the factors above.

Now, solving the case where the drop is being accelerated (region I) by the fall of the hammer. In this region Y(0) = 0 and Y'(0) = 0, however, there is now a pressure gradient across the drop; N = 0. The pressure gradient is taken to be constant since the acceleration of the drop is a constant.

Since

$$N_1' = \frac{N_1}{s}$$

$$N_2' = \frac{N_2}{s}$$

$$N_3' = \frac{N_3}{s}$$

the equation for y can be written as

$$\Delta y = \frac{(N_1 + N_3)(s + 1/\delta_2)}{s(s + \frac{1}{\delta_1})(s^2 + \frac{\delta_1}{\delta_2} + 2\beta)} - \frac{2N_2}{s(s^2 + \frac{\delta_1}{\delta_2} + 2\beta)}$$

This can be solved by taking the inverse Laplace Transform of the above equation, becomes

$$\Delta y(t) = \frac{(1/\delta_1 - 1/\delta_2)e^{-t/\delta_1} 4\delta_2^2 \left[y_1(0) + y_3(0)\right]}{(2\delta_2/\delta_1 - 1)^2 - \gamma^2}$$

$$- e^{-t/2\delta_2} \cosh\frac{\gamma t}{2\delta_2}\left[4\delta_2(\delta_2/\delta_1 - 1)\right]\left[y_1(0) + y_3(0)\right]$$

$$e^{-t/2\delta_2} \frac{\sinh\gamma t}{\gamma} \frac{}{2\delta_2}\left[4\delta_2 y_2(0) - 2\delta_2\left[(2\delta_2/\delta_1 - 1) - \gamma^2\right]\right]$$

The solution for y(t) can be expanded and the first order term can be kept and the rest dropped since, in region I the time t is short compared to δ_1, δ_2 and $1/\gamma$. Upon doing the expansion the coefficient of time is

$$\frac{8\delta_2^2 \ (P_{II} + P_{33})\left[\frac{1}{\delta_2} - \frac{1}{\delta_1}\right]}{f_1 h_1 \ (\frac{2\delta_2}{\delta_1} - 1)^2 - \gamma^2} \ .$$

This gives the value for the difference in the radii of curvature for the drop as it moves through the capillary tube.

Appendix C

Laplace Transforms and Often Used Integrals[13]

Laplace transform methods have been used throughout the derivation of the model to convert a set of coupled differential equations, which can be difficult to solve, to set of algebraic equations, which in principal are easier to solve. Another advantage pf using the Laplace transform method is that the initial value of the function and its time derivative are easily extracted from the solutions.

By definition the Laplace transform of y(t) is

$$L\ y(t) = y(s) = \int_0^\infty e^{-st}\ y(t)\ dt \quad .$$

By definition the inverse Laplace transform of y(s) is

$$L^{-1}\ y(s) = y(t) = \frac{1}{2\pi i} \lim_{T\to\infty} \int_{C-iT}^{C+iT} e^{st}\ y(s)\ ds$$

where C is chosen so that all of the poles of y(s) lie to the left of the line Re s = C in the complex s plane.

The following notation for Laplace transforms is used throughout the dissertation:

function	transform
$y(t)$	$y(s)$
$y'(t)$	$sy(s)-y(0)$
$y''(t)$	$s^2y(s)-sy(0)-y'(0)$
1	$\frac{1}{s}$

where y(0) is the initial value of y(t) (at t = 0) and y'(0) is the value of the time derivative of y(t) at t = 0.

The following integrals have to be evaluated in order to take the inverse Laplace transform so that a solution may be obtained

$$I_o = \frac{1}{2\pi i} \int_{C'} e^{st}\, ds = \frac{1}{s}$$

$$I_1 = \frac{1}{2\pi i} \int_{C'} \frac{e^{st}}{s} ds = 1$$

$$I_2 = \frac{1}{2\pi i} \int_{C'} \frac{e^{st}\, ds}{s\left(s + \frac{1}{\delta}\right)} \quad ds = \delta\,(1 - e^{-t/\delta}) \quad ,$$

where C' is the contour previously indicated for the inverse Laplace transforms. Using $\gamma = 1 - 8\beta\delta_2^2$, we obtain the following;

$$I_3 = \frac{1}{2\pi i} \int \frac{e^{st}\, ds}{s^2 + \frac{s}{\delta_2} + 2\beta}$$

$$= \frac{2\delta_2}{\gamma}\, e^{-t/2\delta_2} \sinh \frac{\gamma t}{2\delta_2}$$

$$I_4 = \frac{1}{2\pi i} \int \frac{e^{st}\, ds}{s\left(s^2 + \frac{s}{\delta_2} + 2\beta\right)}$$

$$= \frac{4\delta_2^2\, e^{-t/2\delta_2}}{\gamma(\gamma^2 - 1)} \left[\gamma \cosh \frac{\gamma t}{2\delta_2} + \sinh \frac{\gamma t}{2\delta_2}\right] + \frac{1}{2\beta}$$

$$I_5 = \frac{1}{2\pi i} \frac{e^{st}(s + 1/\delta_2)\, ds}{s^2 + \frac{s}{\delta_2} + 2\beta}$$

$$= \frac{e^{-t/2\delta_2}}{\gamma} \left[\gamma \cosh\frac{\gamma t}{2\delta_2} + \sinh\frac{\gamma t}{2\delta_2} \right]$$

$$I_6 = \frac{1}{2\pi i} \int \frac{e^{st}\, ds}{s(s + \frac{1}{\delta_1})(s^2 + \frac{s}{\delta_2} + 2\beta)}$$

$$= \frac{\delta_1}{2\beta} - \frac{\delta^3 e^{-t/\delta_1}}{(1 + \frac{\delta_1}{\delta_2} + 2\beta)}$$

$$+ e^{-t/2\delta_2} \cosh\frac{\gamma t}{2\delta_2} \left[\frac{\delta_1^3}{(1 + \frac{\delta_1}{\delta_2} + 2\beta\delta_1^2)} - \frac{\delta_1}{2\beta} \right]$$

$$+ \frac{e^{-t/2\delta_2}}{\gamma} \sinh\frac{\gamma t}{2\delta_2} \left[\frac{\delta_1^3}{(1 + \frac{\delta_1}{\delta_2} + 2\beta\delta_1^2)} - \frac{\delta_1}{2\beta} \right]$$

Appendix D

Mechanics of the Apparatus [14]

The equation for the velocity of the carriage C can be determined by considering seperately the linear motion of the carriage, and the linear motion and the angular rotation of the screw, lever arm and the hammer with mass attached to it.

a) Linear Motion of the Carriage

The forces acting on the carriage are shown in Fig. D 1. Newton's equation for the motion of the carriage of mass m_c having velocity v is

$$m_c \frac{dv}{dt} = F_s - F_{ap} - f \qquad (1)$$

where F_s is the force exerted by the screw on the carriage, F_{ap} is the force due to the air pressure, and f is the frictional force. This frictional force f consists of two terms;

1) the friction due to the carriage sliding on the bars, given by $\mu_{kc} m_c g$, where μ_{kc} is the coefficient of sliding friction.
2) the friction between the teflon pistons and glass given by bv, where b is a constant.

Hence, equation 1 becomes

$$m_c \frac{dv}{dt} = F_s - F_{ap} - \mu_{kc} m_c g - bv \qquad (A)$$

b) Linear Motion of the Screw, Lever Arm and Hammer with Mass Attached to it

The linear acceleration of the screw x_s is given by the equation

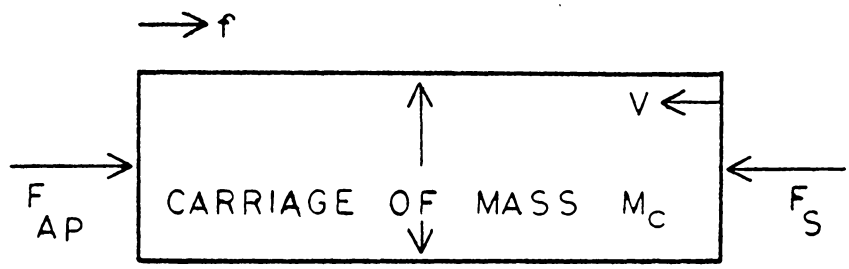

Fig. D.1. Forces acting on carriage of mass m_c.

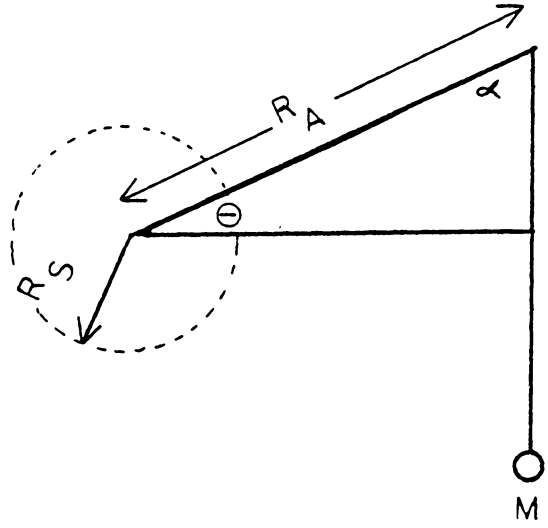

Fig. D.2. Front cross-sectional view of the apparatus.

$$(m_s+m_A+m)\ddot{x}_s = N_H-F_c' \qquad (2)$$

where m_s is the mass of the screw, m_A is the mass of the lever are, m_H is the mass of the hammer, m is the mass attached to the hammer, N_H is the force exerted by the screw threads of the holder H, and F_c' is the force exerted by the carriage on the screw.

But, by Newton's third law, the force exerted by the carriage on the screw is equal and opposite to the force F_s exerted by the screw on the carriage, and thus equation 2 becomes

$$(m_s+m_A+m_H+m)\ddot{x}_s = N_H-F_s \qquad (B)$$

c) Angular Rotation of the Screw, Lever Arm and Hammer with Mass Attached to it

Fig. D 2 shows the cross section of the screw of radius R_s with the lever arm and hammer with mass attached to it. The equation of motion for the angular acceleration $\ddot{\Theta}$ of this screw assuming R_A and α remain constant is

$$\left[I_s+m_A(R_A/2)^2+(m+m_H)R_A^2\right]\ddot{\Theta} = (m+m_H)gR_A\sin\alpha + m_Ag(R_A/2)\sin\alpha- \quad _i \qquad (C)$$

where I_s is the moment of inertia of the screw, R_A is the length of the lever arm, α is the angle between the lever arm and the hammer, and Γ_i is given as

$$\Gamma_i = \quad _{kh}R_sN_H + \mu_{kn}r_{eff}F_s \qquad (D)$$

where μ_{kh} is the coefficient of sliding friction of the screw in the holder H, μ_{kn} is the coefficient of sliding friction of the screw in

the notch N, and r_{eff} is the effective radius of the part of the screw that is in the notch N.

The acceleration of the carriage is equal to the linear acceleration of the screw which in turn is related to the angular acceleration of the screw by the pitch p, so that

$$\frac{dv}{dt} = \ddot{x}_s = p\,\ddot{\theta} \qquad (4)$$

Using this relation, equations A, B, and C can be combined to give the equation of motion of the carriage C as

$$\left\{\frac{1}{p}\left[I_s+m_A(R_A/2)^2+(m+m_H)R_A^2\right]+\mu_{kh}R_s(m_s+m_A+m_H+m)+\mu_{kc}r_{eff}m_c\right\}\frac{dv}{dt}=\left\{(m+mH)gR_A\sin\alpha\right.$$

$$\left. + m_A g(R_A/2)\sin\alpha-\mu_{kh}R_s(F_{ap}+\mu_{kc}m_c g)-\mu_{kc}r_{eff}(F_{ap}+\mu_{kc}m_c g)\right\}-\mu_{kh}R_s bv \quad (D)$$

or

$$\frac{dv}{dt} = \frac{K}{m_{eff}} - \frac{\mu_{kh}R_s bv}{m_{eff}} \qquad (E)$$

where m_{eff} is the curly bracket on the left side of equation D and K is the curly bracket on the right hand side of equation D.

Now K and m_{eff} are of the order of 10^6 and $\mu_{kh}R_s bv$ is of order of 10. The second term on the right hand side of equation E is very small (since m_{eff} is very large) compared to $\mu_{kh}R_s bv$ and hence can be neglected. Thus,

$$\frac{dv}{dt} = \frac{K}{m_{eff}} = a \text{ (constant)} \qquad (F)$$

where a is the acceleration of the carriage.

Equation F was experimentally verified as follows: In equation D the only variables are the mass attached to the hammer, the length R_A of the lever arm and angle α which this lever arm makes with the hammer. By keeping R_A and α fixed and varying M, the acceleration of the carriage can be varied. This was done experimentally and table D.1 shows the values obtained for the acceleration of the carriage with different mass m attached to the hammer.

For the evaluation of equation F, r_{eff} was obtained from equation D, by applying the condition for no turning of the screw. For this case equation D becomes

$$0 = (m+m_A)gR_A\sin\alpha + m_A g(R_A/2) - \mu'_{sh}R_s(F_{ap}+\mu'_{sc}m_c g) - \mu'_{sc}r_{eff}(F_{ap}+\mu'_{sc}m_c g)$$

from which r_{eff} can be found. In the above equation μ'_s are the coefficients of static friction. The agreement between the values obtained from experiment and from evaluation of equation F (theory) is also shown in table D.1.

Thus the acceleration of the carriage can be kept constant by attaching the same mass to the hammer, while the velocity of the carriage can be varied by letting the hammer fall from different heights (this would change the time of fall), for fixed values of R_A and α.

Since the pistons were attached to the carriage they would move with the same velocity v as the carriage while the mercury drop in

the capillary would have a velocity v_m given by:

$$v_m A_m = vA$$

where A_m is the cross-sectional area of the capillary and A is the cross-sectional area of the glass cups.

For evaluating equation E the following values were used:

$I_s = 16.01$ gm-cm^2	Moment if inertia of the screw
$m_s = 142$ gms	Mass of the screw
$R_s = 0.475$ cm	Radius of the screw
$p = 0.15/2$	Pitch of the screw threads
$m_c = 416$ gms	Mass of the carriage including pistons
$m_H = 528$ gms	Mass of the hammer without weights
$m_A = 68$ gms	Mass of the lever arm
$F_{ap} = 6.705 \times 10^6$ dynes	Force due to air pressure of 70 lbs/in^2
$R_p = 0.375$ cm	Radius of teflon pistons
$A_p = 0.44$ cm^2	Cross-sectional area of teflon pistons
$R_c = 0.665$ cm	Radius of air cylinder
$A_c = 1.389$ cm^2	Cross-sectional area of air cylinder
$\mu_{kc} = 1.4$	Coefficient of sliding friction of Al. on Al.
$\mu'_{sc} = 1.05$	Coefficient of static friction for Al. on Al.
$\mu_{kh} = 0.44$	Coef. of sliding friction for steel in brass
$\mu'_{sh} = 0.51$	Coef. of static friction for steel in brass
$\mu_{kn} = 0.44$	Coef of sliding friction for steel in brass
$r_{eff} = 0.0785$ cm	Effective radius of screw in notch N

Table D.1. Values of Acceleration of Carriage and Mass Attached to the Hammer

Mass	Acceleration of Carriage in cm/sec^2	
m in gms	Experiment	Theory
87	1.77	1.915
174	1.85	2.04
261	2.01	2.15
348	2.15	2.28
439	2.30	2.305
530	2.41	2.46

Method for Measuring the Velocity and the Acceleration of the Mercury Drop

Two metal flags were attached to the hammer. These flags were made to pass through the slits in wooden blocks to which a light pipe and a photo diode were inserted in the holes at either side. When the flags pass by the holes they would block the light and change the resistance of the photo diode which in turn would trigger electronic timers. The first would start the timer at the instant the hammer was released from some height and to stop the timer at the instant the hammer came to a stop. Thus, this timer measured the time it took the hammer to drop. Another timer was used to measure the time it took a second flag (0.5 cm. in breadth) to pass the hole, just before the hammer started to deaccelerate. This gave the maximum velocity of the hammer. This velocity of the hammer was related to the maximumdrop velocity by a coupling constant k; which is the ratio of the distance the hammer moved to the distance the drop moved. Thus by knowing the velocity of the drop and the time it traveled the acceleration was computed using equation F of appendix D.

Appendix E

Electrochemistry and Thermodynamics

The following is a study of the electrochemisrty and thermodynamics of a mercury-perchloric acid interface.

Bockris[10] gives, for a metal ion-metal reaction of the form

$$M \rightleftharpoons M^{z+} + Ze^{-} ,$$

where M stands for a metal, Z stands for the number of the charge of the ion, the electrochemical potentials for the reaction have to be equal. Thus,

$$\bar{\mu}_m = \bar{\mu}_{m^{z+}} + z\bar{\mu}_e ,$$

where $\bar{\mu}$'s are the electrochemical potentials. The electrochemical potential is just the chemical potential μ plus a term proportional to the charges, Z, times the inner potential. The three electrochemical potentials are

$$\bar{\mu}_m = \mu_m$$

$$\bar{\mu}_{m^{z+}} = \mu_{m^{z+}} + ZF\phi_s$$

$$\bar{\mu}_e = \mu_e - F\phi_m ,$$

where ϕ_s is the innerpotential of the solution side and ϕ_m is the innerpotential of the metal side. The potential difference across the interface is

$$\Delta\phi_e = (\phi_s - \phi_m) = \frac{1}{ZF}(\mu_{m^{z+}} + \mu_e - \mu_m) = \frac{-\Delta G}{ZF} .$$

The chemical potentials are related to the activities a_i by

$$\mu_i = \mu_i^o + RT \ln a_i .$$

Using this in the expression for $\Delta\varphi_e$ and the usual chemistry convention of $a_m = 1$ for the pure metal and $a_e = 1$ for the free electron, this gives

$$\Delta\varphi_e = \frac{\mu^o_{m^{z+}} + \mu^o_e - \mu^o_m}{zF} + \frac{RT}{zF} \ln a_{m^{z+}} .$$

Following an article by David Turnbull,[15] the Gibbs-Thompson boundary conditions can be developed. With a Gibb's surface of area A seperating two phases α,β with volumes V^α and V^β; the change in the energy of the system is

$$dU = TdS - P^\alpha dV^\alpha - P^\beta dV^\beta + \sum_i \mu_i n_i + \sigma dA ,$$

where σ is the surface tension, μ_i the chemical potential, T is temperature, P is pressure and S is the entropy. Displacing the interface infinitesimally normal to itself at constant total volume, total energy, entropy and composition gives

$$(P^\beta - P^\alpha)dV = \sigma dA .$$

Since

$$\frac{dA}{dV} = \frac{1}{R_1} + \frac{1}{R_2} = K_1 + K_2 ,$$

where K_1 and K_2 are the sums of the two principal curvatures of th surface,

$$P^{\beta}-P^{\alpha} = \sigma(K_1 + K_2)$$

$$= \sigma\left(\frac{1}{R_1} + \frac{1}{R_2}\right) .$$

Looking at a single phase droplet of phase β and radius r, the chemical potential $\mu_{\beta}(r)$ is the same as the bulk phase with a hydrostatic pressure. At a constant temperature for the bulk phase

$$dG = VdP + \sum_i \mu_i dn_i - SdT \quad ;$$

for a single phase $G = n\mu$.

Thus,

$$\frac{dG}{dP} = \frac{d\mu}{dP} = V \ ;$$

Therefore,

$$\mu_{\beta}(r) - \mu_{\beta}(\infty) = \int_{P_{\beta}(\infty)}^{P_{\beta}(r)} V^{\beta} dP \ .$$

Assuming the phase is incompressible, that is, V = constant, gives

$$\mu_{\beta}(r) = \mu_{\beta}(\infty) + V^{\beta}\left[P_{\beta}(r) - P_{\beta}(\infty)\right] \ .$$

Using

$$P_{\beta}(r) - P_{\alpha}(r) = \frac{2\sigma}{r},$$

the following result is obtained:

$$\mu_{\beta}(r) = \mu_{\beta}(\infty) + V^{\beta}\frac{2\sigma}{r} + V^{\beta}(P^{\alpha} - P^{\beta}(\infty)) \ .$$

In applying this result, the chemistry of mercury ions in perchloric acid will have to be investigated.

The chemistry of mercury in an acidic solution has been studied by Edwin Gould.[16] At the interface,

$$Hg \rightleftharpoons Hg^{+} + e^{-} \quad ,$$

which means that mercury and mercury ions reach an equilibrium concentration across the interface. Experiments at 18°C indicate that the mercury present in acidic solution is Hg^{++} , since

$$\frac{[Hg^{++}]}{[Hg_2^{+}]} = 116 \quad .$$

According to Bockris,[10] the Butler-Volmer equation describes the behavior of currents and potentials at the interface. The equation can be derived by looking at the current passing through the interface. Figure 1 shows the interface region including the inner and outer helmholtz layers. Following Bockris,[10] the current passing from the metal to the solution shaould be

$$i_{m\rightarrow s} = (kT/n)\, C^{M}_{Hg^{o}}\, e^{\frac{-\Delta G^{o}}{kT}}\, (2e)\, e^{\frac{\beta e(\varphi^{o}+\eta)}{kT}} \quad ,$$

and passing from the solution to the metal is

$$i_{s\rightarrow m} = (kT/n)\, C^{s}_{Hg^{+}}\, e^{\frac{-\Delta G^{o}}{kT}}\, e^{\frac{-\Delta G'}{kT}}\, (2e)\, e^{\frac{-\beta' e(\varphi^{o}+\eta)}{kT}} \quad .$$

The net current is

$$i_{sm} = i_{m\rightarrow s} - i_{s\rightarrow m}$$

$$= \frac{2ekT}{n}\, e^{\frac{-\Delta G^{o}}{kT}} \left[C^{M}_{Hg^{o}}\, e^{\frac{\beta e(\varphi^{o}+\eta)}{kT}} - C^{s}_{Hg^{+}}\, e^{\frac{-\Delta G'}{kT}}\, e^{-\beta' e(\varphi^{o}+\eta)} \right] \quad .$$

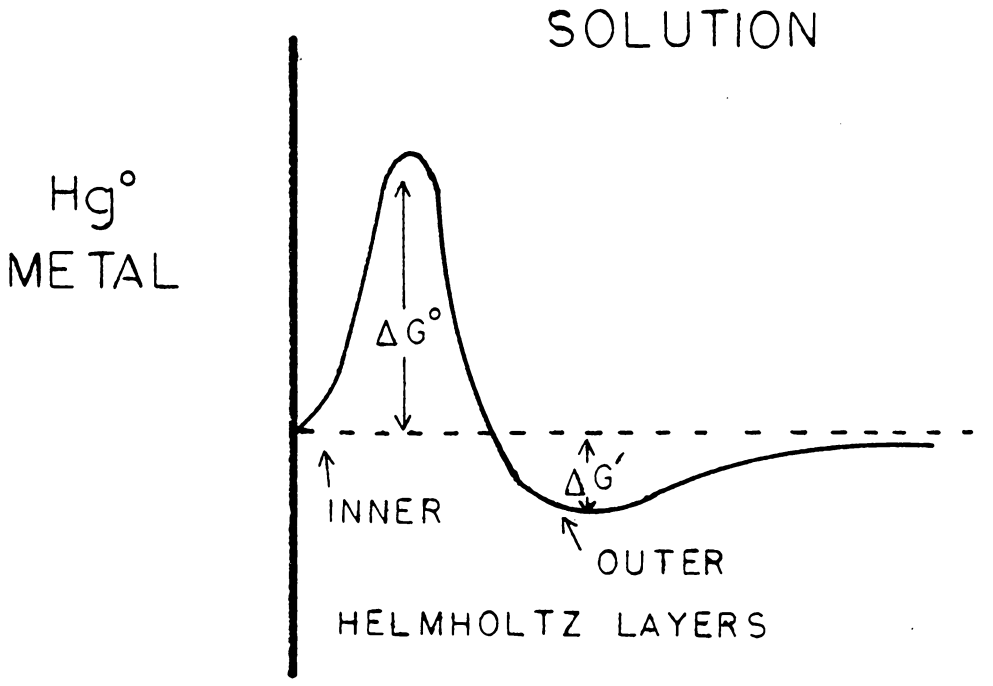

Fig. E.1. Diagram of interface showing the inner and outer Helmholtz layers.

Assuming the surface has a capacitance, the net current through the interface would be

$$i = C_M \frac{d\eta}{dt} + i_{sm}(\eta, t) \quad ,$$

where η is the overpotential and φ^o is the equilibrium potential difference across the interface. $C^s_{Hg^o}$ is the surface concentration of ions on the metal, $C^s_{Hg^+}$ is the surface concentration of the ions in the solution phase, and ΔG isthe free energy. The potential difference across one of the metal solution interfaces is $\varphi^o + \eta$. Since the external current is zero in the experiments,

$$0 = C_M \frac{d\eta}{dt} + i_{sM}(\eta, t) \quad .$$

Because this equation is homogeneous, the η is expected to decay to zero. Using i_o to define the equilibrium exchange current we obtain

$$0 = C_m \frac{d\eta}{dt} + i_o\left[e^{\frac{\beta e \eta}{kT}} - e^{\frac{-\beta' e \eta}{kT}}\right]$$

or

$$0 = \frac{d\eta}{dt} + \frac{e i_o (\beta+\beta')}{C_m kT}\eta$$

$$= \frac{d\eta}{dt} + \frac{\eta}{\tau} \quad ,$$

where

$$\frac{1}{\tau} = \frac{e i_o (\beta+\beta')}{C_m kT} \quad .$$

Appendix F

The data for the experiment is given in this section. Table F1. gives the data for voltage versus velocity, tablr F2. gives the data for the electrochemical relaxation time, tables F3. through F8. gives the data for voltage versus time for different drop sizes, table F9. gives the effective decay constant versus drop length, and table F10. gives data for acceleration versus velocity for different acceleration weights. The following values are used throughout the experiment and model to calculate different parameters.

Surface Tension = 370 dynes/cm^2

Density of Mercury = 13.3 gm/cm^3

Density of Acid = 1.07 gm/cm^3

Tube Diameter = 1.0 mm

Viscosity of Mercury = 1.95×10^{-2} cm/gm/sec

Viscosity of Acid = 1.078×10^{-2} cm/gm/sec

Capacitance of Layer = 16 microfarad/cm^2

TABLE F1. DATA FOR VOLTAGE VERSUS VELOCITY

Drop length = 1.7 cm acceleration = 51.2 cm/sec^2

	Velocity (cm/sec)	Voltage (mV)		Velocity (cm/sec)	Voltage (mV)
	1.96	80		3.56	150
	2.00	78		3.50	145
	2.02	85		3.60	145
	1.95	78		3.55	142
	1.98	79		3.60	142
	1.96	80		3.55	147
average	1.98	80	average	3.56	147
	4.70	186		5.85	240
	4.74	185		5.95	240
	4.80	180		5.79	235
	4.81	180		6.05	230
	4.70	190		6.06	225
	4.69	189		6.00	240
average	4.74	185	average	5.95	240
	7.70	305		8.30	333
	7.80	309		8.80	328
	7.82	315		8.60	330
	7.95	310		8.35	355
	8.00	320		8.45	360
	7.65	301		8.48	340
average	7.82	310	average	8.50	341

TABLE F1 (continued)

	Velocity (cm/sec)	Voltage (mV)
	10.2	400
	10.2	390
	10.0	385
	10.0	405
	10.7	415
	10.0	405
average	10.2	400

Average Values (Standard Deviation)

Velocity (cm/sec)	Voltage (mV)
1.98(.03)	80(2.6)
3.56(.04)	145(3.1)
4.74(.05)	185(4.3)
5.95(.11)	235(6.3)
7.82(.14)	310(6.8)
8.50(.18)	341(13.5)

TABLE F2. DATA FOR ELECTROCHEMICAL RELAXATION TIME

Number of drops	Ratio (Volts/Amps)
25	3.18×10^6
22	3.18×10^6
19	3.18×10^6
16	3.18×10^6
13	3.07×10^6
11	2.82×10^6
8	2.57×10^6
6	2.33×10^6
4	2.06×10^6
2	1.84×10^6
1	1.59×10^6

Slope = 1.089×10^5 ohms

$i_o(Hg) = 4.408 \times 10^{-7}$ amps

$\frac{1}{\delta} = 1.368 \times 10^{-2} = .01368$ seconds

TABLE F3. VOLTAGE VERSUS TIME

0.745 cm drop

Region III

Time (secs)	Volt (mV)	Volt (mV)	Volt (mV)	Volt (mV)	Volt (mV)	Volt (mV)	Volt (mV)	Volt (mV)
0.0	-157	-160	-155	-155	-165	-157	-155	-155
0.045	170	165	170	180	170	170	175	170
0.075	200	210	200	200	195	200	200	195
0.1	180	175	180	200	175	170	180	180
0.17	130	125	140	125	130	130	125	135
0.24	75	75	70	75	73	78	75	70
0.295	39	40	38	40	35	40	42	40
0.335	26	25	30	25	24	26	25	26

Average Values
Region III

Time (secs)	Volt (mV)	Volt Calc.
0.0	-157(4)	-157
0.045	171(4)	178
0.075	200(5)	200
0.1	180(9)	185
0.17	130(5)	126
0.24	74(3)	74
0.295	39(2)	37
0.335	26(2)	24

$$V = -157\, e^{-183t} + 1.48 \times 10^{4}\, e^{-13.5t} \sinh(0.5t)$$

$$\frac{1}{\delta_o} = 13.0$$

Region I

Time (secs)	Volt (mV)	Slope (volts/sec)
0.055	200	3.64
0.058	210	3.62
0.055	200	3.64
0.053	200	3.77
0.058	220	3.79
0.056	210	3.75
0.058	200	3.45
0.055	205	3.73

average slope = 3.67(.11)

TABLE F4. VOLTAGE VERSUS TIME

1.139 cm drop

Region III

Time (secs)	Volt (mV)	Volt (mV)	Volt (mV)	Volt (mV)	Volt (mV)	Volt (mV)	Volt (mV)	Volt (mV)
0.0	-137	-140	-140	-135	-135	-140	-133	-137
0.03	40	40	35	50	40	35	40	42
0.07	60	60	60	60	55	58	65	62
0.08	60	60	60	55	60	60	60	58
0.105	58	55	60	58	57	58	60	55
0.15	47	50	45	45	50	48	47	48
0.21	30	30	28	30	30	30	35	30
0.26	20	20	20	20	20	20	20	20
0.31	15	13	15	18	15	13	16	15
0.36	10	10	10	9	10	12	10	10
0.425	6	5	6	5	5	6	8	6

Average Values
Region III

Time (secs)	Volt (mV)	Volt Calc.
0.0	-137(3)	-137
0.03	40(5)	39
0.07	60(3)	59
0.08	59(2)	60
0.105	58(2)	58
0.15	47(2)	47
0.21	30(2)	33
0.26	20(0)	21
0.31	15(2)	14
0.36	10(1)	10
0.425	6(1)	5

average slope = 2.58(.13)

$$V = -137\, e^{-171t} + 784\, e^{-12.6t} \sinh(2.6t)$$

$$\frac{1}{\delta_o} = 10.0$$

Region I

Time (secs)	Volt (mV)	Slope (Volts/sec)
0.085	200	2.35
0.08	210	2.63
0.08	200	2.5
0.078	210	2.69
0.083	230	2.77
0.08	200	2.5
0.08	210	2.63
0.079	200	2.53

TABLE F5. VOLTAGE VERSUS TIME

1.765 cm drop

Region III

Time (secs)	Volt (mV)	Volt (mV)	Volt (mV)	Volt (mV)	Volt (mV)	Volt (mV)	Volt (mV)	Volt (mV)
0.0	-195	-190	-200	-200	-195	-190	-195	-200
0.065	59	60	60	60	55	58	60	60
0.120	70	70	75	70	70	75	70	68
0.2	60	60	60	60	65	58	58	60
0.345	30	30	25	30	30	30	30	30
0.54	13	15	10	15	12	13	10	13
0.74	3	5	1	3	3	1	3	2

Average Values
Region III

Time (secs)	Volt (mV)	Volt Calc.
0.0	-196(4)	-196
0.065	59(2)	59
0.12	71(3)	70
0.145	67(2)	68
0.2	60(2)	60
0.345	29(2)	30
0.54	13(2)	11
0.74	3(1)	3

$$V = -196\, e^{-116t} + 1722\, e^{-8.4t} \sinh(1.8t)$$

$$\frac{1}{\delta_o} = 7.5$$

Region I

Time (secs)	Volt (mV)	Slope (volts/sec)
0.066	200	3.03
0.05	200	4.00
0.058	200	3.45
0.058	200	3.45
0.06	200	3.33
0.06	210	3.50
0.058	200	3.45
0.058	205	3.53

average slope = 3.47(.27)

TABLE F6. VOLTAGE VERSUS TIME

4.101 cm drop

Region III

Time (secs)	Volt (mV)	Volt (mV)	Volt (mV)	Volt (mV)	Volt (mV)	Volt (mV)	Volt (mV)	Volt (mV)
0.0	-270	-260	-275	-275	-265	-270	-280	-270
0.04	38	35	40	40	35	40	35	38
0.1	56	55	57	55	60	55	65	55
0.11	57	57	60	60	55	60	57	58
0.13	55	55	55	55	57	55	57	55
0.23	44	45	45	40	45	43	45	45
0.33	28	30	25	25	30	28	30	26
0.43	17	20	15	15	20	17	18	17
0.48	12	10	15	12	13	12	13	12

Average Values
Region III

Time (secs)	Volt (mV)	Volt Calc.
0.0	-271(6)	-271
0.04	38(2)	37
0.1	57(4)	57
0.11	58(2)	58
0.13	55(1)	56
0.23	44(2)	42
0.33	28(2)	27
0.43	17(2)	16
0.48	12(2)	12

$$V = -271e^{-116t} + 173\, e^{-8.4t}\sinh(2.9t)$$

$$\frac{1}{\delta_o} = 5.5$$

Region I

Time (secs)	Volt (mV)	Slope (volts/sec)
0.075	340	4.53
0.075	340	4.53
0.08	340	4.25
0.08	340	4.25
0.075	340	4.53
0.07	320	4.57
0.07	320	4.57
0.08	345	4.31

average slope = 4.44(.15)

TABLE F7. VOLTAGE VERSUS TIME

6.873 cm drop

Region III

Time (secs)	Volt (mV)	Volt (mV)	Volt (mV)	Volt (mV)	Volt (mV)	Volt (mV)	Volt (mV)	Volt (mV)
0.0	-235	-240	-240	-230	-225	-235	-235	-240
0.035	56	55	50	60	55	56	55	55
0.085	93	90	95	90	90	95	95	93
0.13	105	100	100	110	108	105	104	107
0.185	90	95	93	95	90	96	100	90
0.285	70	75	75	70	65	75	75	70
0.385	50	50	50	45	50	53	50	50
0.485	30	35	30	30	35	30	30	30
0.53	28	25	30	30	28	30	25	30

Average Values
Region III

Time (secs)	Volt (mV)	Volt Calc.
0.0	-235(5)	-235
0.035	55(3)	56
0.085	93(2)	96
0.13	105(4)	104
0.185	94(4)	96
0.285	72(4)	73
0.385	50(2)	49
0.485	31(2)	32
0.53	28(2)	27

$V = -235\, e^{-116t} + 586\, e^{-8.4t} \sinh(3.9t)$

$\frac{1}{\delta_o} = 4.5$

Region I

Time (secs)	Volt (mV)	Slope (volts/sec)
0.055	200	3.64
0.055	200	3.64
0.055	200	3.64
0.057	200	3.51
0.055	200	3.64
0.055	200	3.64
0.057	200	3.51
0.057	200	3.51

average slope = 3.59(.07)

TABLE F8. VOLTAGE VERSUS TIME

7.818 cm drop

Region III

Time (secs)	Volt (mV)	Volt (mV)	Volt (mV)	Volt (mV)	Volt (mV)	Volt (mV)	Volt (mV)	Volt (mV)
0.0	-100	-95	-100	-110	-95	-105	-105	-90
0.045	73	70	75	80	70	70	75	70
0.1	105	100	103	105	109	105	97	111
0.13	108	110	105	112	105	109	106	109
0.145	105	100	102	106	109	105	100	108
0.25	80	80	75	75	90	80	81	78
0.36	60	60	55	55	68	60	60	60
0.46	37	35	40	37	35	40	35	36
0.565	24	25	20	25	25	25	23	25

Average Values
Region III

Time (secs)	Volt (mV)	Volt Calc.
0.0	-100(6)	-100
0.045	73(4)	72
0.1	104(5)	105
0.13	108(3)	108
0.145	104(3)	106
0.25	80(5)	83
0.36	60(4)	58
0.46	37(2)	37
0.565	24(2)	25

$V = -100\ e^{-116t} + 586\ e^{-8.4t}\sinh(4.0t)$

$\frac{1}{\delta_o} = 4.4$

Region I

Time (secs)	Volt (mV)	Slope (volts/sec)
0.065	280	4.31
0.068	290	4.26
0.07	295	4.21
0.073	300	4.11
0.073	285	3.90
0.065	265	4.08
0.07	285	4.07
0.07	290	4.14

average slope = 4.14(.13)

TABLE F9. EFFECTIVE DECAY CONSTANT
VERSUS
DROP LENGTH

Effective Decay Constant (sec^{-1})	Experimental Drop Length (cm)	Calculated Drop Length (cm)
13.0	0.745	0.851
10.0	1.139	1.14
7.5	1.765	1.75
5.5	4.101	4.08
4.5	6.873	6.88
4.4	7.818	7.82

$$\frac{1/\delta_o}{1/2\delta_2} = 1.195 - \sqrt{1.0 - 0.629/L}$$

TABLE F10. FATA FOR ACCELERATION VERSUS VELOCITY FOR DIFFERENT WEIGHTS

Number of Weights	Acceleration (cm/sec/sec)	Velocity (cm/sec)
5	33.0	7.7
	29.0	6.3
	32.0	6.5
	29.0	5.2
	30.0	4.7
	27.0	3.4
3	18.2	4.61
	17.3	2.68
	16.8	2.24
1	11.3	3.29
	11.0	3.10
	12.9	2.80
0	6.20	2.40
	5.7	2.10
	7.4	1.7
2	17.0	3.6
	13.0	4.3
	16.0	2.8
	14.0	1.6

TABLE F10. (continued)

Average Values of Weights versus Acceleration

Number of Weights	Acceleration (cm/sec/sec)
5	30.0(2.2)
3	17.0(0.7)
2	15.0(1.8)
1	12.0(1.0)
0	6.4(0.8)

Appendix G

The following is the two mass - one spring problem which represents a single interface. This problem will not give quantitative agreement since the coupling terms; are not all in one equation as in the model used; however, it should show the general characteristics as seen in the experiment. Figure G.1. shows the system from which the following equations are obtained;

$$m_1\ddot{x}_1 = -\frac{m_1\dot{x}_1}{\delta_1} - k(x_1 - x_2 + a) \qquad (1a)$$

$$m_2\ddot{x}_2 = -\frac{m_2\dot{x}_2}{\delta_2} + k(x_1 - x_2 + a) \quad . \qquad (1b)$$

Let $y_1 = x_1 + a$ and $y_2 = x_2$; thus, equations 1 becomes

$$\ddot{y}_1 + \frac{\dot{y}_1}{\delta_1} + \omega_1^2 (y_1 - y_2) = g_1(t) \qquad (2a)$$

$$\ddot{y}_2 + \frac{\dot{y}_2}{\delta_2} + \omega_2^2 (y_2 - y_1) = -g_2(t) \quad . \qquad (2b)$$

After taking the Laplace transform of the above equations and placing them in matrix form and allowing the initial condition terms to vanish, the following is obtained

$$\begin{bmatrix} f_1 + \omega_1^2 & -\omega_1^2 \\ -\omega_2^2 & f_2 + \omega_2^2 \end{bmatrix} \begin{bmatrix} y_1(s) \\ y_2(s) \end{bmatrix} = \begin{bmatrix} g_1(s) \\ -g_2(s) \end{bmatrix}$$

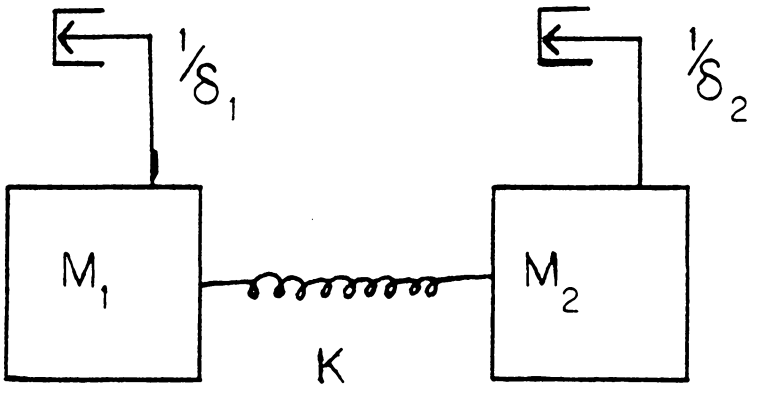

Fig. G.1. Two mass system from which the equations for Appendix G.

where $f_1 = s(s + 1/\delta_1)$ and $f_2 = s(s + 1/\delta_2)$. For simplicity in solving for the zero's of the determinant δ_1 will be set equal to δ_2. Multiplying through by the inverse of the determinant and solving for $y(s) = y_2(s) - y_1(s)$ giving

$$\Delta y(s) = \frac{f\left[g_1(s) + g_2(s)\right]}{(f+\omega_1^2)(f+\omega_2^2) - \omega_1^2\omega_2^2}$$

$$= \frac{g_1(s) + g_2(s)}{\left[s + \frac{1}{2\delta} - \Omega\right]\left[s + \frac{1}{2\delta} + \Omega\right]}$$

where $\Omega = \sqrt{(1/2\delta)^2 - \omega_1^2\omega_2^2}$.

The inverse Laplace transform can be taken and the value of $y(t)$ can be obtained. Figure G.2 gives a series of curves showing $y(t)$ versus time for different relative values of T_1 (the time the acceleration force is turned off) and T_2 (the time the deacceleration is turned on). For our case $T_1 = T_2$, which is the third graph. Notice the basic feature are the same as the experiment. The overall sign comes from how $\Delta y(t)$ is defined.

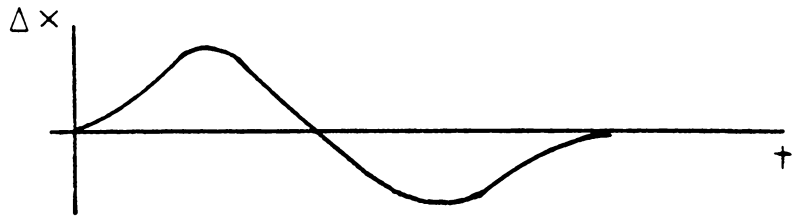

a) $T_1 = \frac{T_2}{2} = \frac{T_3}{3}$

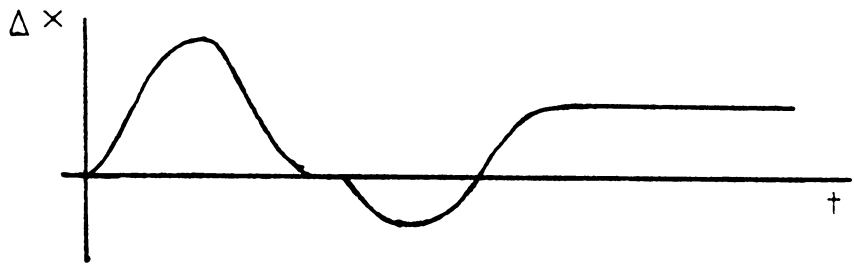

b) $T_1 > T_2$

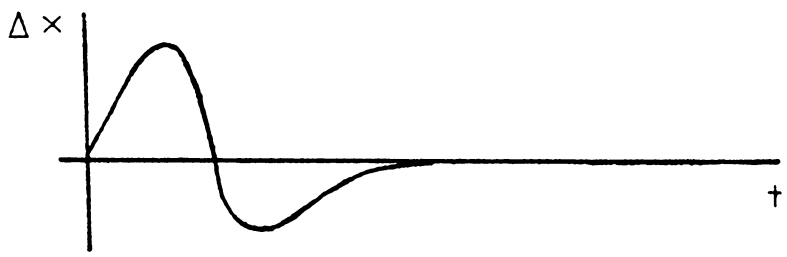

c) $T_1 = T_2$

Fig. G.2. Figures show solutions for the equations for different values of T_1, T_2, and T_3.

BIBLIOGRAPHY

1. Ueda, S., Watanabe, A., Tsuji, F.

   J. Electrochem. Soc. Japan 19, 142 and 153, 1951

   J. Electrochem. Soc. Japan 20, 605, 1952

   J. Electrochem. Soc. Japan 21, 14, 1953

2. Ueda, S., Tsuji, F., Watanabe, A.

   Int. Cong. of Surf. Activity, Proc. 2nd, London 3 3, 1957

3. Elliot, R., Packard, R., Kyeazis, D.

   College of Medicine, Univ. of Cincinnati, Circulation 9, Feb., 1954

4. Fain, W., Brown, S., Lockenwitz, A.

   J. Acous. Soc. Amer. 29, 902, 1957

5. Podolsky, B., Kuskevics, G., Rivers, J.

   J. Applied Physics 28, 357, 1957

6. Bamji, S. S., Bowen, S. P., Tipsword, R. F.

   Phys. Chem. Liq. 8, 189, 1978

7. Kotowski, J., Koczorowski, Z., Figaszewski, Z.

   J. Applied Electrochem. 10, 179, 1980

   J. Applied Electrochem. 10, 185, 1980

   J. Applied Electrochem. 10, 191, 1980

   J. Applied Electrochem. 10, 197, 1980

8. Landau, L. D., Lifshitz, E. M.

   Fluid Mechanics, Pergamon Press, 1959

9. White, F. M.

Viscous Fluid Flow, 1974

10. Bockris, J. O'M., Reddy, A. K.

Modern Electrochemistry, Plenum Press, N. Y. Volume 1, 1970

Modern Electrochemistry, Plenum Press, N. Y. Volume 2, 1970

11. Martin, P. C.

Measurement and Correlation Functions in Many Body Physics Gordon and Breach, N. Y., 1968

12. Levich, V. G.

Physicochemical Hydrodynamics, 1962

13. Spiegel, M. R.

Mathematical Handbook, Schaum's Outline Series, 1968

14. Bamji, S. S.

Ph.D. Thesis, Virginia Tech., 1976

15. Turnball, D.

Solid State Physics 3, 225, 1956

16. Gould, E. S., Hold, H.

Inorganic Reactions and Structure, 1955

17. Lamb, H.

Hydrodynamics, Dover, 1932

18. Gibbs, J. W.

Collected Works, Volume 1, 1931

19. Tolman, R. C.

J. Chem. Phys. 16, 758, 1948

J. Chem. Phys. 17, 118 and 333, 1949

20. Buff, F. P.

J. Chem. Phys. 19, 1591, 1951

21. Herring, C.

Structures and Properties of Solid Surfaces, Univ. Chicago Press, 1953

22. Cushing, J. T.

Applied Analytical Mathematics for Physical Scientists, Wiley and Sons, N. Y., 1975

23. Mortimer, C. E.

Chemistry A Conceptual Approach, Reinhold, N. Y., 1967

The vita has been removed from the scanned document

VOLTAGES PRODUCED AT THE POLARIZED MERCURY-ELECTROLYTE INTERFACE

by

Robert C. Mania Jr.

(ABSTRACT)

The electrical potential differences which arise across the length of capillary tubes containing 1 N perchloric acid and mercury drops are studied experimentally and theoretically for constant acceleration and different lengths of the drops of mercury. A relatively simple theory explains many features of the voltage on the experimental parameters. The results suggests that surface modes exist on the mercury drops which, in association with the Gibbs-Thompson effect, is the coupling between the mechanical and electrochemical phenomena.